UMTRI-2007-4

Vibration Transmission from Road Surface Features – Vehicle Measurement and Detection

Technical Report

for
Nissan Technical Center North America, Inc.

by
Timothy J. Gordon
Zevi Bareket

The University of Michigan
Transportation Research Institute (UMTRI)
2901 Baxter Road, Ann Arbor, MI 48109-2150

January 2007

Technical Report Documentation Page

1. Report No.	2. Government Accession No.	3. Recipient's Catalog No.
UMTRI-2007-4		

4. Title and Subtitle	5. Report Date
Transmission from Road Surface Features – Vehicle Measurement and Detection	January 2007
	6. Performing Organization Code 567010
7. Author(s) Gordon, T., Bareket, Z.	8. Performing Organization Report No. UMTRI-2007-4
9. Performing Organization Name and Address The University of Michigan Transportation Research Institute (UMTRI) 2901 Baxter Road, Ann Arbor, MI 48109-2150	10. Work Unit No. (TRAIS)
	11. Contract or Grant No. DRDA 06-0002 (N006540/382841)
12. Sponsoring Agency Name and Address Nissan Motors Corp.	13. Type of Report and Period Covered Final Technical Report
	14. Sponsoring Agency Code

15. Supplementary Notes

16. Abstract

This report documents the results of extensive vehicle-based measurements on a Nissan Infiniti Q56 Sports Utility Vehicle, for the purpose of vibration source characterization. A sophisticated sensor and data acquisition system was fitted to a Nissan Infiniti Q56 Sports Utility Vehicle, supported by simultaneous video and CAN data recording. The question studied was whether the captured signals are sufficient to form the basis of a reliable and robust rumble strip detection system. The instrumentation and data analysis were not supposed be representative of such a product-specific system, but were configured as a research tool to support the future development of such a system. Signal analysis showed that a subset of the accelerometers provided information for detection. Further analysis of the production wheel-speed sensor indicates that it should be able to provide equivalent information, and, with suitable signal processing, provide the basis of a production feasible detection system.

17. Key Word	18. Distribution Statement
Rumble strips, Vibration, Warning systems, Automatic detection, Lane departure, Lane keeping, Suspension, Detection system	

19. Security Classif. (of this report)	20. Security Classif. (of this page)	21. No. of Pages	22. Price
None	None	50	

Table of Contents

Executive Summary

This report describes an experimental study of vehicle vibration response from road surface features, in particular the vibration response from a wide variety of rumble strips. A sophisticated sensor and data acquisition system was fitted to a Nissan Infiniti Q56 Sports Utility Vehicle, supported by simultaneous video and CAN data recording. The system was rigorously calibrated and tested under known conditions, and then over 100 road tests were made with the specific intention of recording and characterizing the range of data generated by rumble strips as well as other road surface features. The general question studied is whether the captured signals are sufficient to form the basis of a reliable and robust rumble strip detection system capable of sensing contact with a rumble strip, discriminating between left and right shoulder rumble strips whatever their mode of construction, and doing so within a sufficiently short period of time that would allow a warning or other safety countermeasure system to operate in real time. The instrumentation and data analysis were not supposed be representative of such a product-specific system, but were configured as a research tool to support the future development of such a system.

Engineering judgment was used to locate eighteen candidate sensors on the vehicle – vertical and longitudinally mounted accelerometers (g-sensors) on both the sprung and unsprung masses at each wheel station (16 sensors) with the addition of two laterally oriented accelerometers on each end of the steering linkages. Of these 18 signals, only the longitudinal accelerations at the unsprung mass provides a reliable measure of the road surface excitation, and these signals are shown to provide sufficient information to determine the presence of rumble strips and reject background vibration sources found on normal highways, dirt roads etc. The lack of national US or other international standards in rumble strip design does not adversely affect the ability of these sensors to recognize rumble strip presence, though the task would be immensely easier if constant pitch spacing were adopted by the highway community.

The information presented by the production wheel-speed sensor appears to be equivalent to that of the preferred g-sensor, in terms of its response to rumble strip features. However, this conclusion is currently tentative since the wheel speed signal was not available in its raw form during this study. Signal processing used for purposes of ABS control reduces the information available on the CAN bus, in which form it is not suitable for detection. In spite of this, indications are that the wheel speed sensor output – suitably processed for the current application – will provide suitable input data for a robust and reliable system for rumble strip sensing by the vehicle.

1. Introduction

The purpose of the project was to investigate which sensor outputs strongly correlate with road surface features, for the purpose of reliable discrimination between different types of road feature. The intention was to reliably identify the vibration characteristics associated with rumble strips at the road edge, and discriminate these special features from other road surface irregularities such as potholes, raised line markings and reflectors (cats eyes).

The project was comprised of two phases:

- ***Phase 1 – Install Vibration Measurement System*** *[March – July 2005]*
  In Phase 1, a data acquisition system, incorporating sensors, amplification, signal conditioning and data recording was fitted to the vehicle. An interface was also provided to the vehicle Control Area Network, to record additional data relevant to the detection issue. Acquisition of forward and rear-pointing video images was also included. Tests were conducted to verify system performance, accuracy and reliability.
- ***Phase 2 – Vehicle Testing (main test program)*** *[August 2005 – March 2006]*
  In Phase 2, a 'library' of relevant road surface features has been compiled, including confounding features such as potholes. A comprehensive set of examples has been identified within South-East Michigan and Ohio, and measurements are currently being conducted to record the vibration responses over these features under a variety of test conditions.

This report, provided at the conclusion of Phase 2, documents the work done during both phases of the project. Phase 1 work is described in Section 1, the vibration measurement system. summarize content

2. Vibration Measurement System

The testing platform that was used in this study was a vehicle that was supplied by Nissan *(Infiniti QX56).* In order to capture, record, and later to analyze the data, a measurement system was designed and installed in the vehicle. This measurement system was comprised of:

- Vibration-measuring sensors (accelerometers)
- Visual capturing system (video cameras)
- Data-recording and monitoring system (DAS)

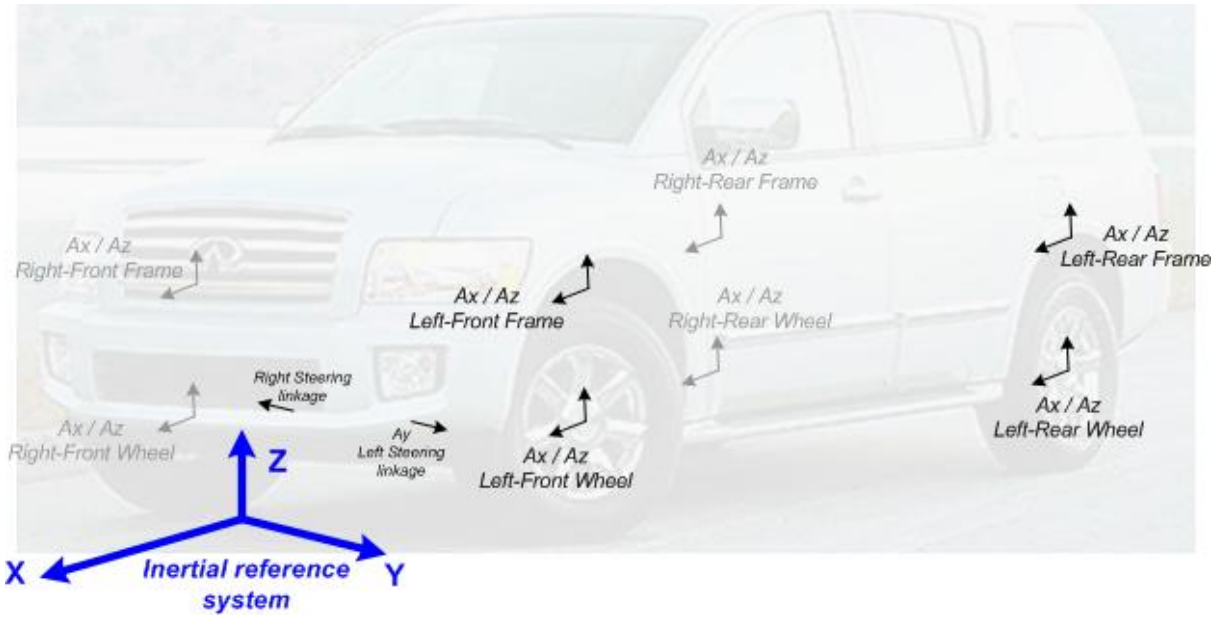

Figure 2.1. Axis system and summary of accelerometers installation

A total of 10 accelerometers have been installed. Two accelerometers were installed on the steering tie rod, one at each end. These accelerometers were single-channel units, and they measured the acceleration that prevailed along the tie rod (which is lateral relative to the direction of travel). Each accelerometer recorded A_y data.

The intent behind installing these accelerometers was to record and analyze the extent of which the significantly different tire-road conditions (one side on the rumble strip while the other side on the pavement) affect steering vibrations. Figure 2.2 shows the accelerometer installation to the right-side of the steering tie rod.

Figure 2.2. Accelerometer installation at the right-side of the steering tie rod

The other eight accelerometers were installed at the four corners (left-front, right-front, etc.) of the vehicle. Each corner had two dual-channel (A_x and A_z) accelerometers: one was installed on the suspension arm to capture unsprung-mass accelerations, and the other one was installed on the frame above it to capture the corresponding sprung-mass accelerations. From the vibration-dynamics standpoint, the hardware installation attempted to capture the dynamic data as illustrated in figure 2.3.

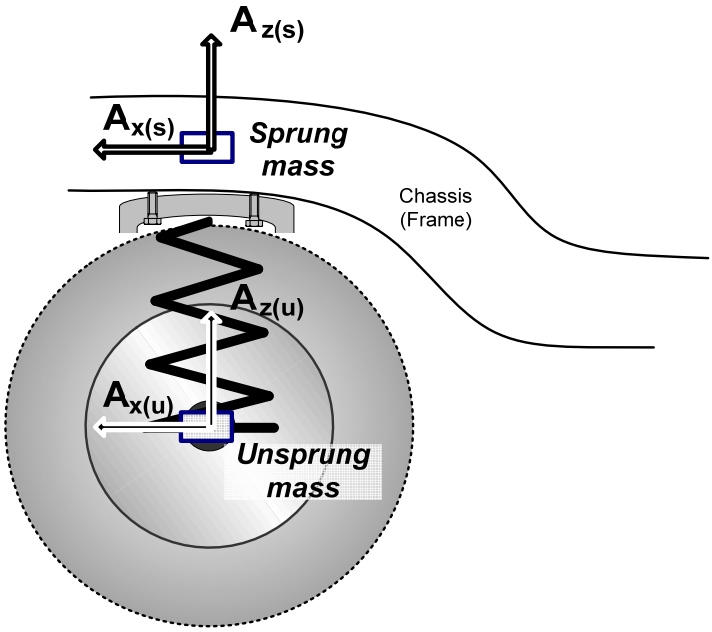

Figure 2.3. Quarter-car model for recording of acceleration data

The figures on the following pages show typical installation of accelerometers for recording sprung- and unsprung-mass vibration data.

Figure 2.4. Right-front accelerometer installation (unsprung-mass data)

Figure 2.5. Right-front accelerometer installation (sprung-mass data)

Figure 2.6. Left-rear accelerometer installation (unsprung-mass data)

The ten accelerometers were wired to the Data Acquisition System (DAS), mounted at the rear of the vehicle (see figure 2.7). Accelerometers data were recorded at 1000 Hz.

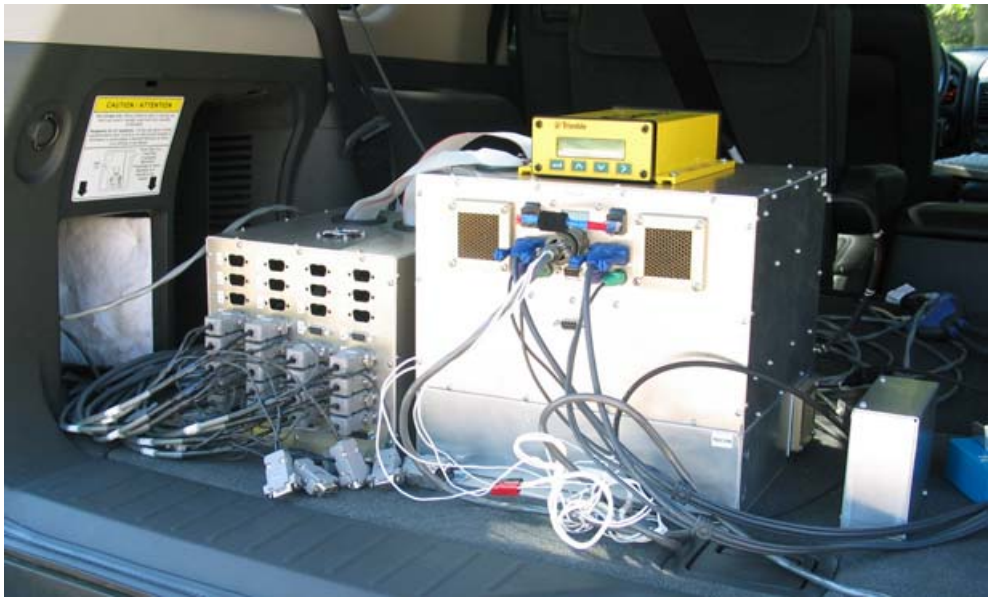

Figure 2.7. Data acquisition system

In addition to the accelerometers, the DAS also records the following items:

- CAN data signals –
    - four wheels rotational speed
    - steering wheel angle
    - vehicle speed
    - vehicle yaw rate

- vehicle longitudinal acceleration
- brake pedal state
- drive mode (4x4/4x2)

- Video –
  - Left- or right-side road camera looking at the contact area between the front wheel and the pavement (side is switched in preparation to each specific test, an image from a road camera is shown further down in this document). Figure 2.8 shows the left-side camera installation.

Figure 2.8. Left-side camera

  - Forward-looking camera to provide contextual information about the test (an image from this camera is shown further down in this document). Figure 2.9 shows the camera installation.

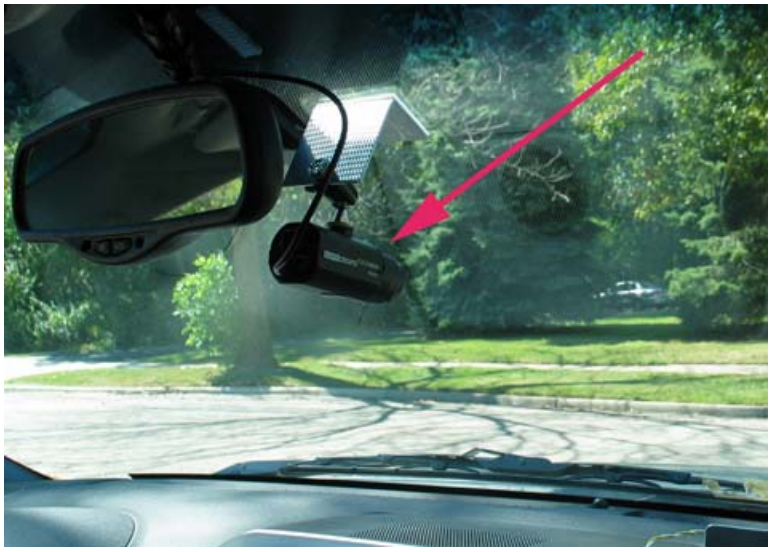

Figure 2.9. Forward-looking camera

- GPS data (speed, location, etc.) The GPS unit is shown in figure 2.7 (the yellow box on top of the DAS).

Controlling the test was done from a “command station” (see figure 2.10). This command station is comprised of a keyboard/mouse unit, and a monitor that is attached to the back of the passenger seat. The operator initializes and stops the data-collection process while seated in the back.

Figure 2.10. Command station and interface

3. Vehicle testing

3.1 Summary of Calibration and Validation Tests

The orientation and zero-reading of the accelerometers had to be validated so that data analysis could later be performed using correct polarity of the appropriate signals. To calibrate and validate the data, two methods were employed: (1) taking measurements on a known level surface, and (2) taking measurements while subjecting the accelerometers to specific external inputs.

3.2 Rumble Strip Types

Raised-paint strips: commonly used across the lane as a warning to the driver of an approaching stop sign and/or intersection. It usually spans about 15 ft.

Figure 3.1. Raised-paint rumble strips

Rolled-in rumble strips: these rumble strips are typically generated by pressing depressions in hot asphalt shoulders or concrete during construction and reconstruction projects.

Figure 3.2. Rolled-in rumble strips (on the right: an intermittent type on concrete)

Milled-in rumble strips: the milled rumble strips are deeper and wider than rolled rumble strips, and they can be installed on new or existing pavements and on both asphalt or concrete shoulders.

Figure 3.3. Milled-in rumble strips

3.3 Example Tests

The complete list of all the tests that were performed is provided in Appendix A. This section provides a detailed description of an example test scenario and its results. Here the vehicle was driven in the left lane, and then steered off to the left past the lane marker and onto the rumble strip. Figure 3.4(a) is a snapshot image from the forward-scene video, and figure 3.4(b) is an image from the left-side road video, depicting the wheel as it crosses the lane marker and before it gets on the rumble strip.

Figure 3.4 (a). Snapshot from forward-scene video

Figure 3.4 (b). Snapshot from the left-side road video

Figure 3.5 shows the CAN data for this test. The time axis is in milliseconds since the DAS was started. At about t=1.93e6 one can observe the left steer input, heading towards the left-side ruble strip.

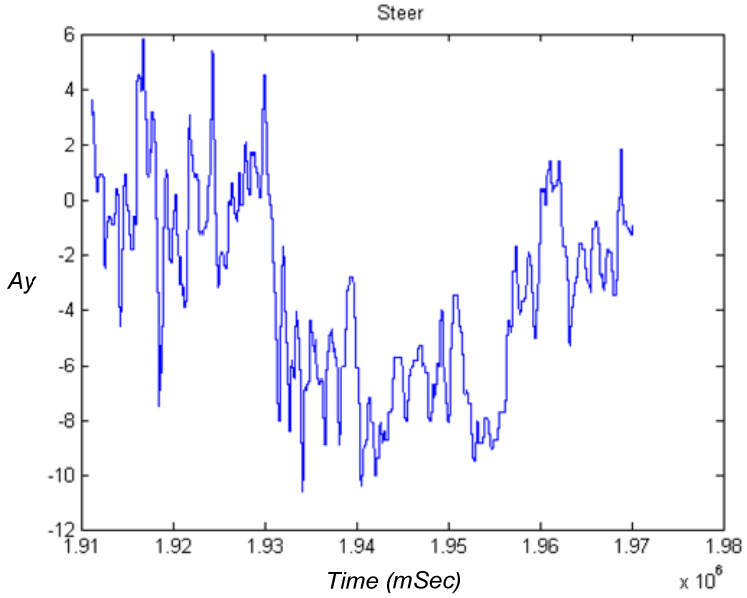

Figure 3.5. CAN Data of steering input

Figure 3.6 depicts the front-wheels Az data (from the suspension-mounted accelerometers), zoomed around the time period that the left wheel get onto the rumble strip. The left side clearly shows higher values of vertical acceleration.

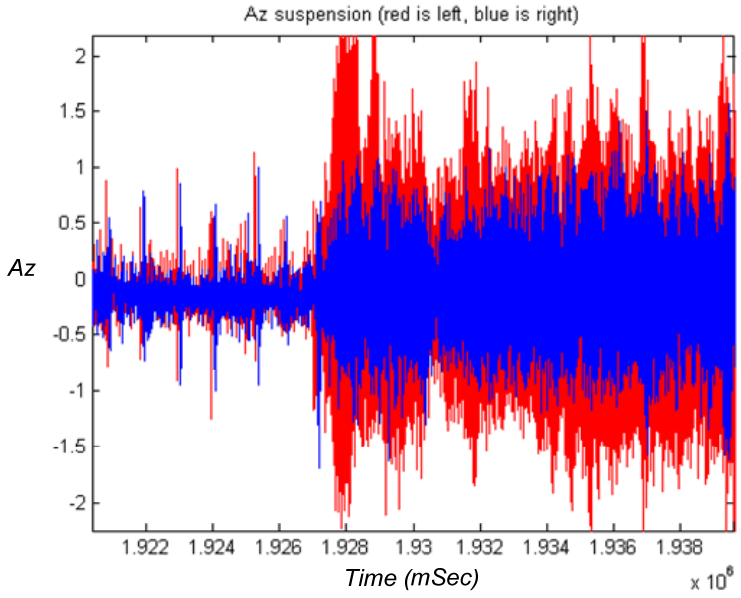

Figure 3.6. Az data, left-front wheel

The next figure shows Ay data from the accelerometer mounted on the steering connecting rod. The whole test duration is shown. The bands of small Ay correspond to the time where the wheels were off he rumble strip, and the large-Ay data correspond to the time where the left wheels get on the rumble strips.

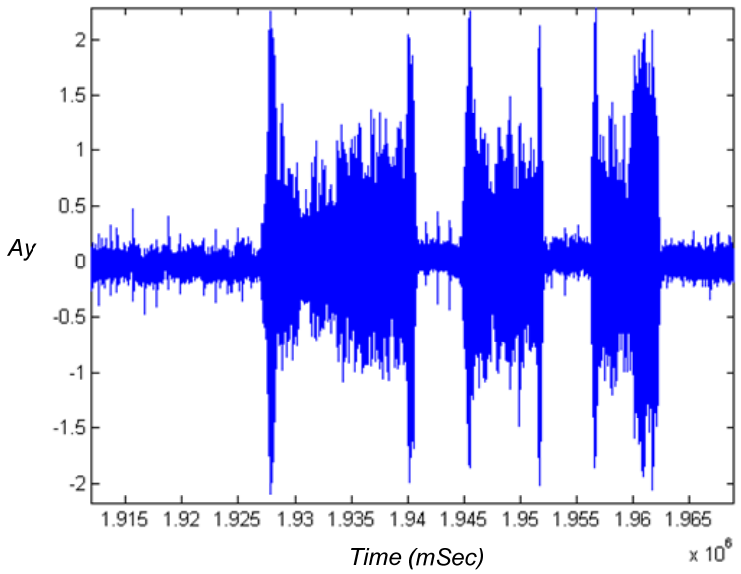

Figure 3.7. Ay data from the steering-linkage accelerometer

The effect of suspension dampening on the vertical acceleration is shown in the next figure. Again, this figure is zoomed around the time where the left wheel gets onto the rumble strip. The red line is the Az data from the left-front wheel (lower suspension arm), and the blue line depicts the data from the frame-mounted accelerometer located above that wheel.

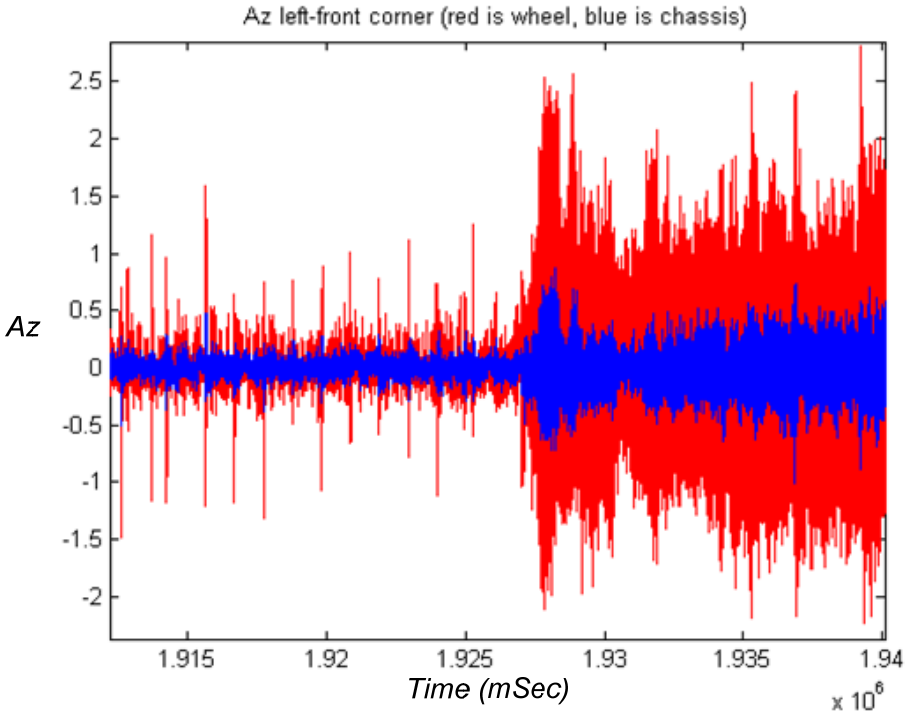

Figure 3.8. Az data from the left-front wheel and chassis

4. Analysis Techniques

A variety of analysis methods were applied to the collected data. In the proposal, these were to be grouped according to the number of variables employed – univariate, bivariate and multivariate. Extensive analysis was employed in the area of single and two variable studies, and the result of these analyses are presented in Section 5 below. As it became clear that the most interesting and relevant results were already available from that part of the study, multivariable analysis in the form of multiple regression and ANOVA – though interesting from an academic perspective – was essentially dropped in favor of a more detailed analysis of using wheel speeds as a sensor that would replace the accelerometers. This has major consequences for possible product development, since the wheel-speed sensor is already available, though (as will be seen in Section 6) it does not yet provide the required information in a useable form. In this section the main methods are summarized in compact equation form. The actual Matlab code used to generate the results is not presented here, but is prepared separately as part of the project deliverables.

4.1 Univariate

The experiments in this study consisted of driving the vehicle at constant speed on rumble strips and other features, as detailed in the appendices. The results of the experiments consist of acceleration variables $a_i(t, j)$ where $i = 1,...,18$ defines the sensor location, t is a time vector recorded at 1kHz on the vehicle, and $j = 1,...,110$ identifies the event (or run). For each run a variety of factors $F_i(j)$ were varied. Again these are detailed in the Appendix, but they may be seen in Figure 4.1 on the right, which is a search window for the online analysis tool used in this project.

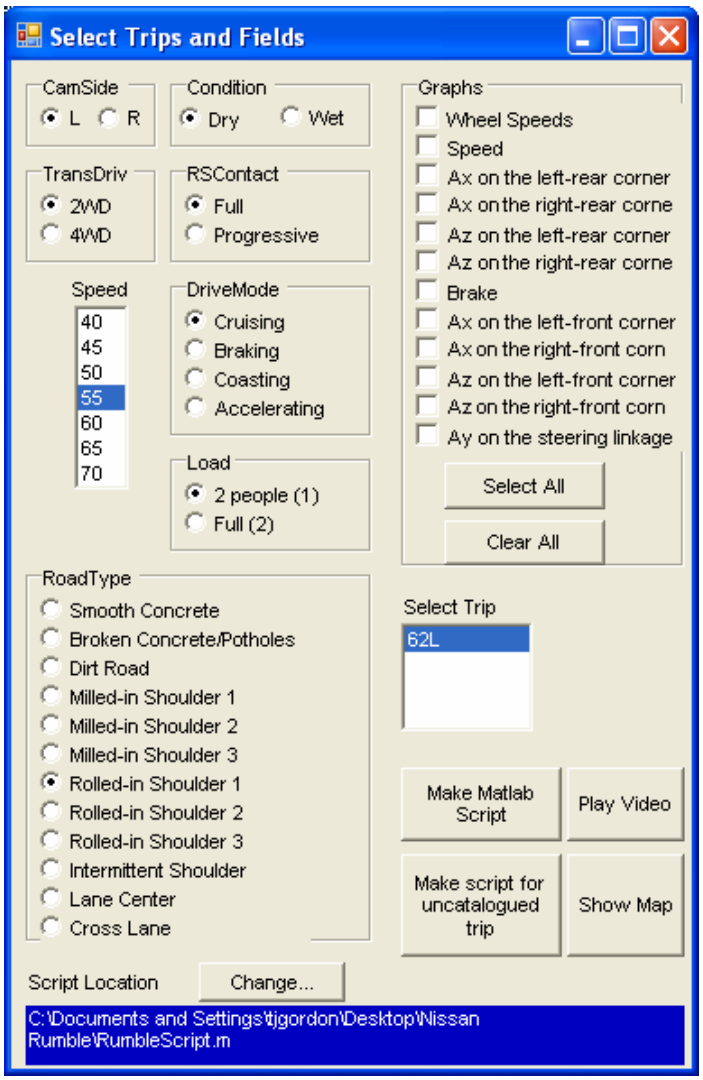

Figure 4.1. Screen-shot from the Online Analysis

There were six major factors of interest:

- Excitation (camera) Side – *left* or *right*
- Road Type – 8 options actually uses (see Appendix)
- Transmission selection – *2WD* or *4WD*
- Driving Mode – for example coasting or in driver (see Figure 4.1)
- Speed
- Rumble Strip Contact – some examples were taken of partial contact, so that the possibility of early detection may be known, as the tire is only partially touching the strip.

Three basic techniques were applied

- Basic plotting and histograms – visual comparison of time history plots, i.e. plotting $(t, a_i(t, j))$ for different values of *i* and *j*.
- Statistical measures of time histories – in particular estimating the effect of a particular factor or combination of factors by calculating the root-mean-square (RMS) of each signal, and averaging over all runs that meet the condition. The condition is of the form: $c = \{F_{i1} \in S_1, F_{i2} \in S_2, ..., F_{ip} \in S_p\}$ which might for example be "the road type should be a milled rumble strip, the speed must be 55mph, and the transmission should be in 2WD". RMS values for all runs $R(c)$ that meet this condition are then averaged and plotted as bar charts to provide a visual map of how the vehicle responds to different inputs under different conditions.
- Fourier analysis. Base on the above techniques, certain signals were seen as being of greater interest, and their frequency characteristics – in form of Discrete Fourier Transforms – are plotted. The result is typically a broadband power spectrum (or Power Spectral Density – PSD) with peaks that occur at the frequencies $f = \{f_0, 2f_0, 3f_0, ...\}$, where $f_0 = \frac{U}{L}$ is the fundamental excitation frequency determined by the rumble strip periodicity *L* and the vehicle speed *U*. Other peaks may occur at frequencies that are speed dependent, for example at resonant frequencies of the tire or the suspension. This is a critical issue, since fixed resonances are likely to occur under a wide range of excitation conditions, while the harmonics $\{f_0, 2f_0, 3f_0, ...\}$ are essentially a signature of the excitation that we seek to detect.

4.2 Bivariate

In this class of analysis, plots were made that explicitly compared the interaction between two factors. Again three types of analysis were carried out

- Waterfall plots – this relationship is possible when data is obtained from coast-down testing, i.e. the vehicle coasts from high to low speed while in contact with a rumble-strip. The power spectrum is plotted multiple times as the speed reduces. This gives a critical measure of the relevant contributions in the response signal between the input signal and the response resonances. The former change frequency in proportion to the vehicle speed (see above) while the latter are fixed by the dynamics of the tire and suspension.
- Factor differences – in this case two sets of factor conditions (c_1, c_2) are chosen as above (e.g. c_1 might be low speed motion on a right-side milled rumble strip, while c_2 is the same set of conditions at high speed) and the comparison between the two sets of conditions is mapped across the sensor set in the form of the difference between the mean RMS values under those conditions.
- Coherency and transfer function estimation in the frequency domain – here the coherency function (or more correctly the squared coherency function) is a frequency dependent measure of linearity between two variables, typically two measured vehicle variables. In this way it can be established whether the two variables are linearly related and hence one can be modeled in terms of the other using linear differential equations, or equivalently via a transfer function. (Because such a model is actually based on frequency data the "transfer function" is more correctly described as an estimated frequency response function.). Thus where high coherency levels can be demonstrated – at least around the frequencies of major excitation – the transfer function can be estimated and used to confirm relationships between different parts of the data. This turned out to be highly significant in the relationship between (partially) measured wheel speeds and measured acceleration responses.

5. Results

This section presents key results from the analysis and summarizes the significance of each result. With a large amount of data captured, very many plots can be generated. Here we limit attention to those of greatest interest to the detectability problem. The results are grouped here by type rather than by number of variables – we start with time histories, move onto factor analysis and finish with frequency analysis.

5.1 Time Histories

Typical time histories were presented in Section 3 above. Here we note some basic features of the time histories and postpone factor analysis to Section 5.2. Figure 5.1 shows a short interval of accelerations on a left-side rumble-strip, where the sub-plots are draw in the same layout as on the vehicle – upper plots are for the front of the vehicle, lower plots for the rear wheels; left side plots correspond to the left wheels, and similarly for the right side plots.

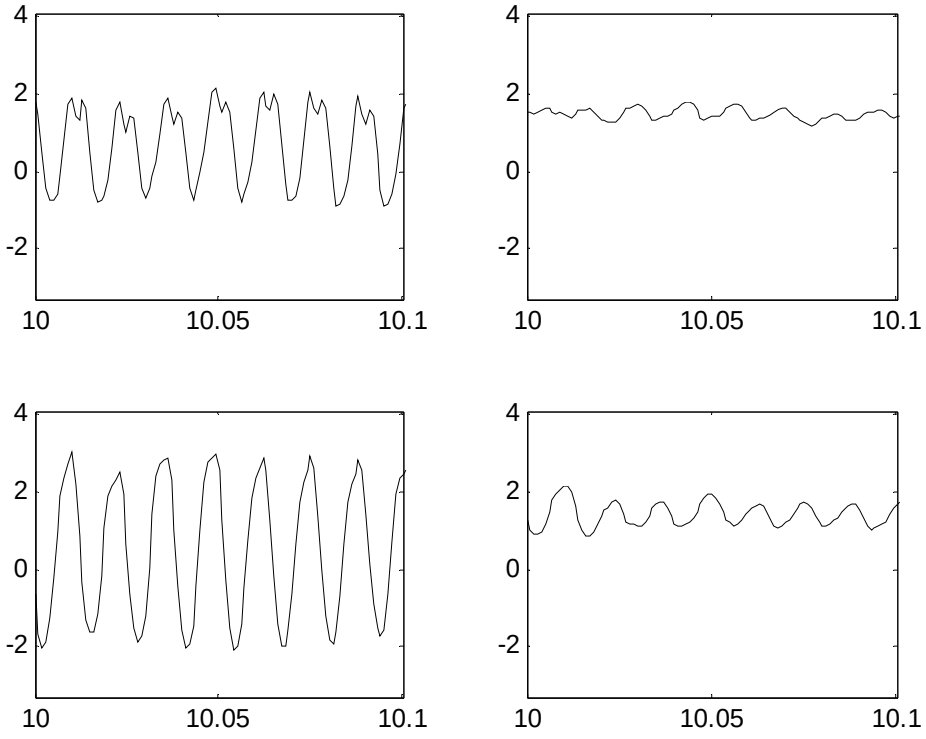

Figure 5.1. Typical Time History – left side rolled-in rumble strip, vertical acceleration at the wheel.

As would be expected, the larger amplitude is on the left (close to he excitation) and each variable is roughly periodic, with a period of approximately 10ms in this case. Note that a

number examples were analyzed in detail to confirm the fundamental period T is indeed related to the rumble-strip length L and vehicle speed U by the relation $T = \frac{L}{U}$ (this may be obvious, but it was considered worth of checking). While the excitation is roughly periodic, the response is far from sinusoidal, exactly as would be expected – each signal is essentially a sum of harmonics, based on the excitation frequency. Contributory effects from the tire and suspension would essentially be to amplify or suppress these harmonics as the frequency varies, and this may cause a problem for detectability (more will be observed on this later). For now, the main conclusion is that the rumble strip excitation is being detected by the vehicle sensors in a way that would be expected, and that the time history information is relatively simple – essentially consisting of a number of harmonic amplitudes that are roughly constant across time. Hence amplitude (RMS) and frequency-based analysis are sufficient to characterize the steady-state response on the rumble strip.

On the other hand, the relative amplitudes of different sensors is not always intuitively so obvious. Figure 5.2 shows a slightly more complex set of responses measured on the chassis from a right-sided rolled-in rumble strip.

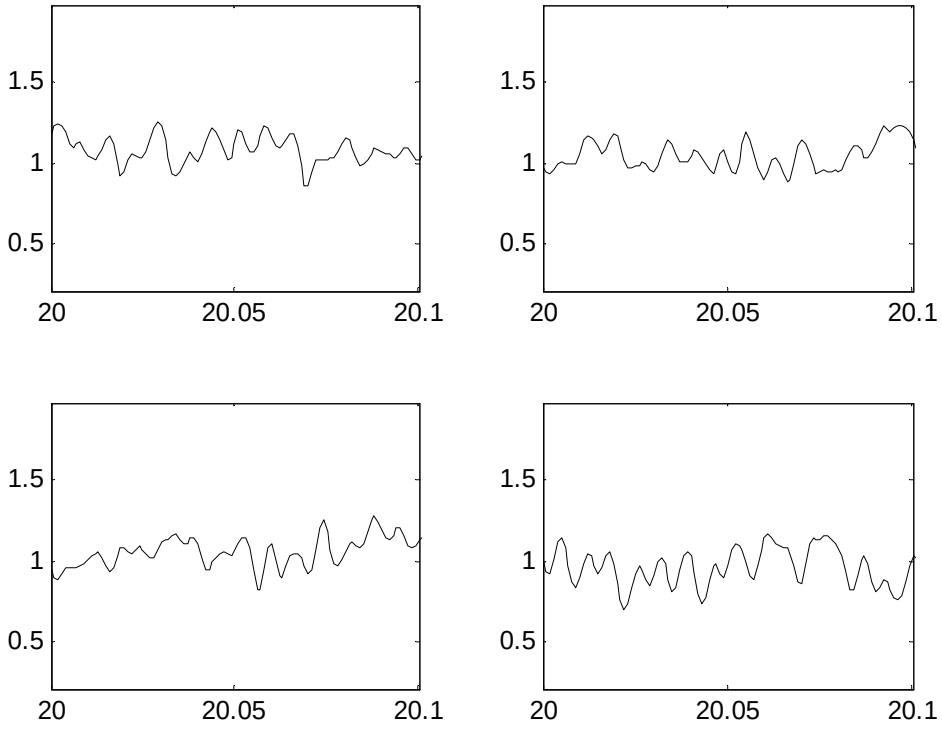

Figure 5.2. Time History of a Right-side rolled-in rumble strip (70mph, vertical acceleration on the chassis side).

The excitations on the right side are not particularly greater than on the left, and it is possibly only the greater approximation to a periodic signal that suggests the excitation was on the right side. As we shall see in the next section, the wheel mounted sensors are considerably more useful as indicators of the location of the rumble strip, and the above is not an isolated result.

With this in mind, and pre-empting one of the key results of Section 5.2, we now consider how one particular sensor signal - $a_{x\,wheel}(t)$ - detects a transition as the vehicle drifts onto the rumble strip. Figure 5.3 shows how the measured acceleration gradually increases as the tire moves onto the rumble strip. Note that the amplitudes (not shown here) on the left side remain small, and the front wheel also shows the same kind of transition. Thus, with the right sensor or sensor to detect the rumble strip, the early effect of partial contact should provide a method of detecting the rumble strip at an early stage.

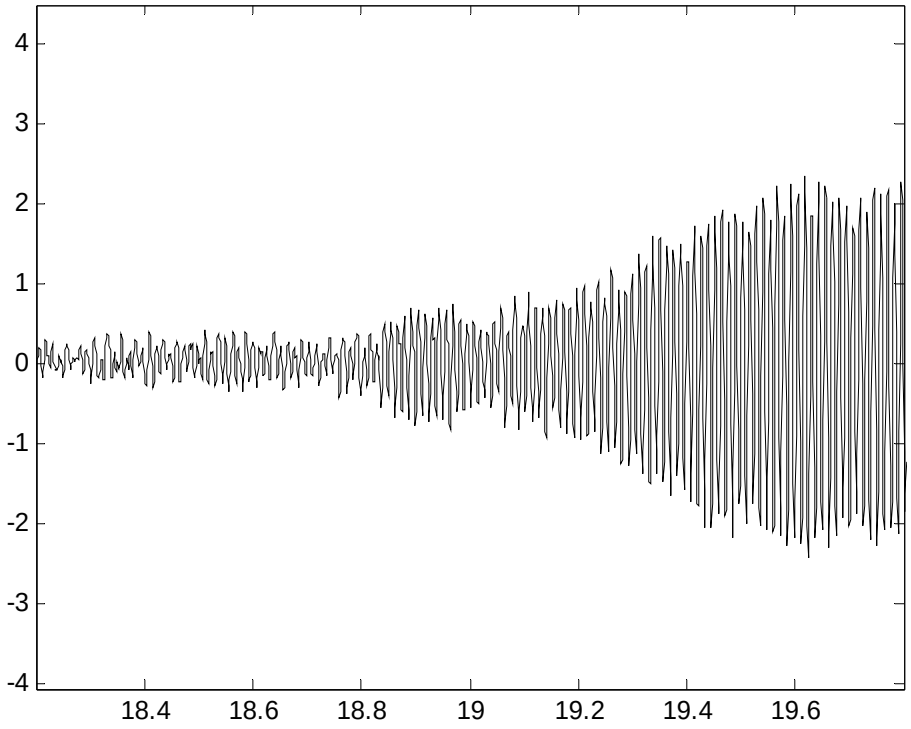

Figure 5.3. Time history of a right-side milled-in rumble strip as the tire progressively contacts the strip (Run 117, 55mph, longitudinal acceleration at the outboard accelerometer, right-rear wheel).

5.2 Factor Analysis Using RMS responses

This analysis focused on the RMS values determined from each of the vibration sensors. Figure 5.4 shows a typical result, the bars presenting RMS accelerations averaged over all cases of interest, in this case averaged over all occasions where a left-side rumble strip (rolled or milled) was tested.

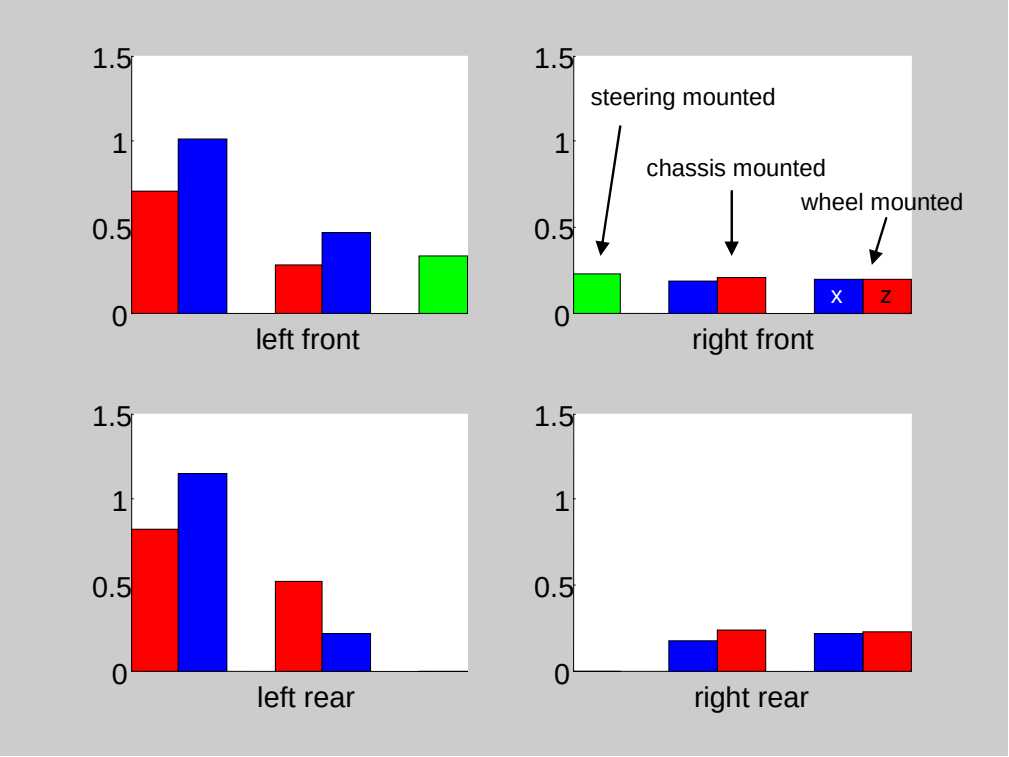

Figure 5.4. Mean RMS Values for all Left Side Rumble Strips

For consistency, and to avoid the effects of partial contact and varying times on the rumble strip, each 'event' analyzed was chosen to be the 10 second interval that generated the largest RMS value. In the following plots, each sub-plot corresponds one corner of the vehicle, red bars represent the vertical (Z) direction, blue bars are for longitudinal (X) and green bars (front only) display the lateral (Y) acceleration on the steering arm. The outer bars represent wheel hub responses, while the chassis mounted accelerometers are shown inboard –intended to be intuitively easy to study the plots. The amplitudes shown clearly represent an expected left-sided bias, though the amplitudes of the chassis mounted accelerometers show a relatively weak effect.

Figure 5.5 shows corresponding right-side responses, and then Figures 5.6 and 5.7 present separate results for milled and rolled-in rumble strips (right-side only since the left side plots are not surprisingly very similar). From these plots it is clear that rolled-in rumble strips present a more difficult problem for detection via chassis mounted accelerometers than milled rumble strips.

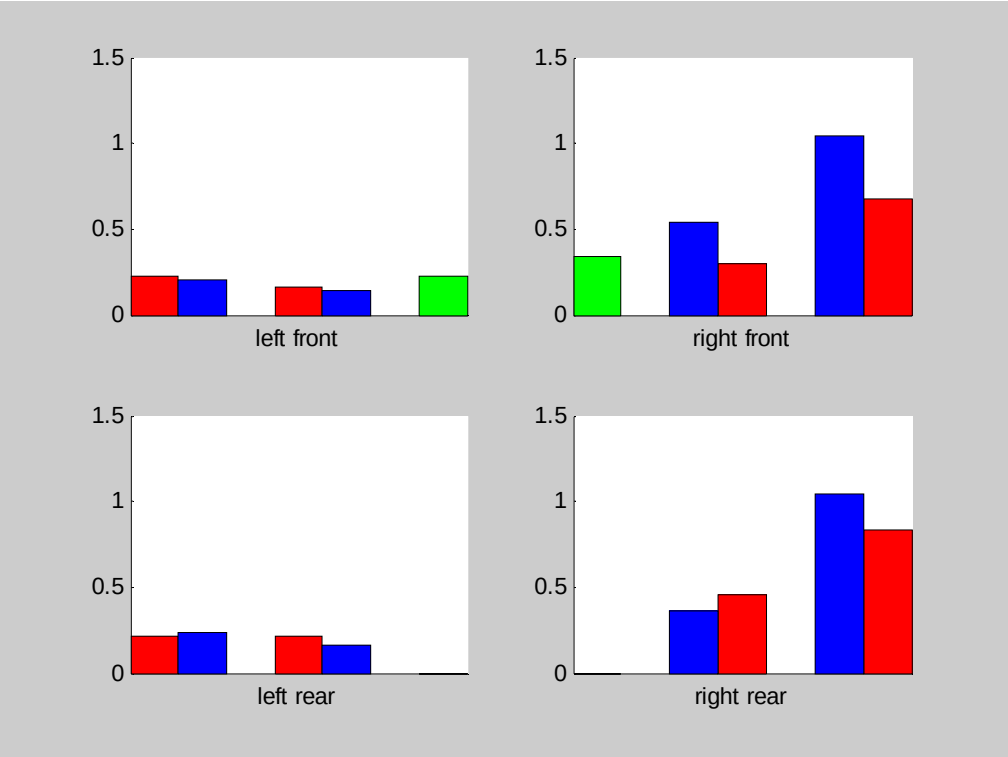

Figure 5.5. Mean RMS Values for all Right Side Rumble Strips

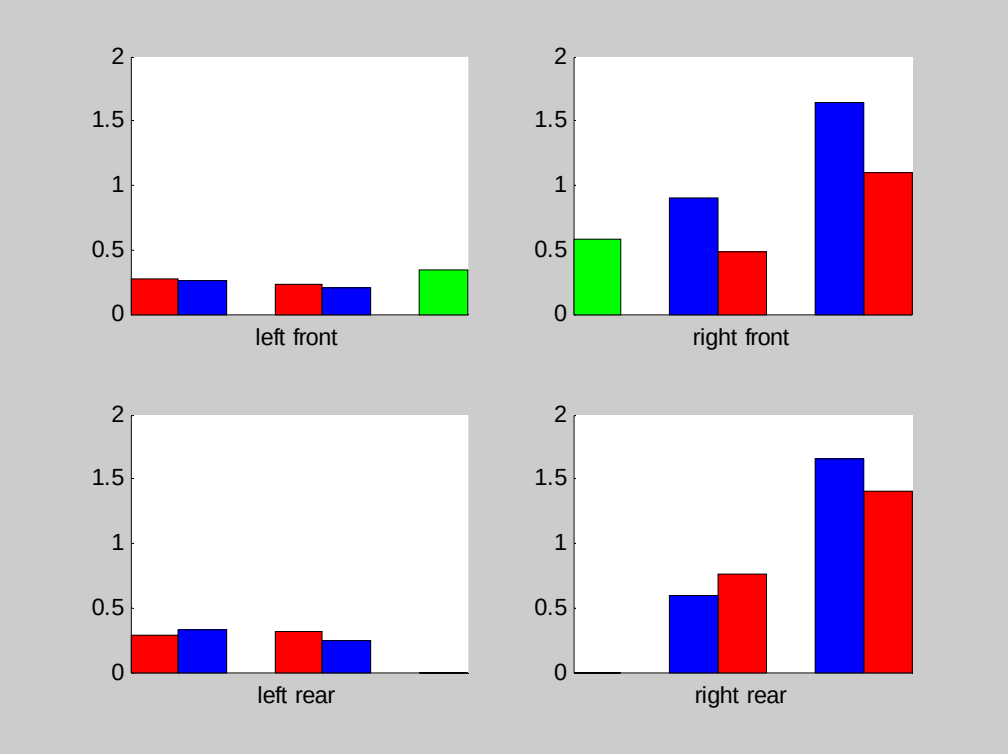

Figure 5.6. Mean RMS Values for Milled Right Side Rumble Strips

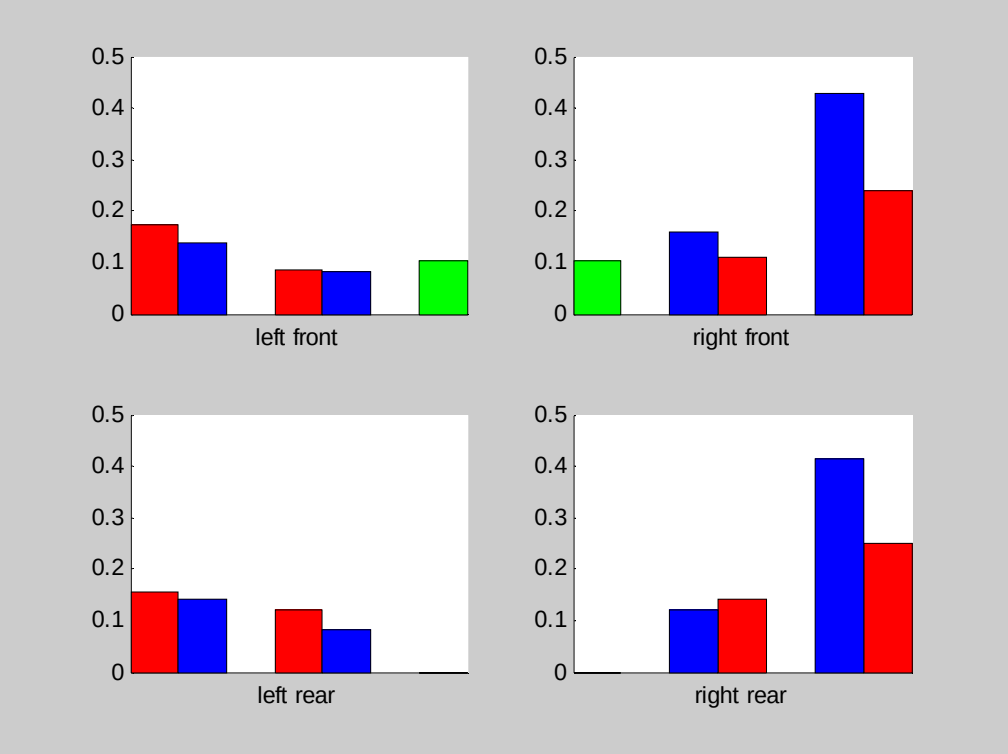

Figure 5.7. Mean RMS Values for Rolled-in Right Side Rumble Strips

Comparing left and right rumble strip responses for the rolled-in case, Figure 5.8 shows the difference in response amplitude. While it might be possible to use relative phase or multivariable information to improve the detection, it is absolutely clear that the outboard (hub mounted) a_x accelerometer is the strongest signal and the best single sensor for detecting both the existence and location of the rumble strip.

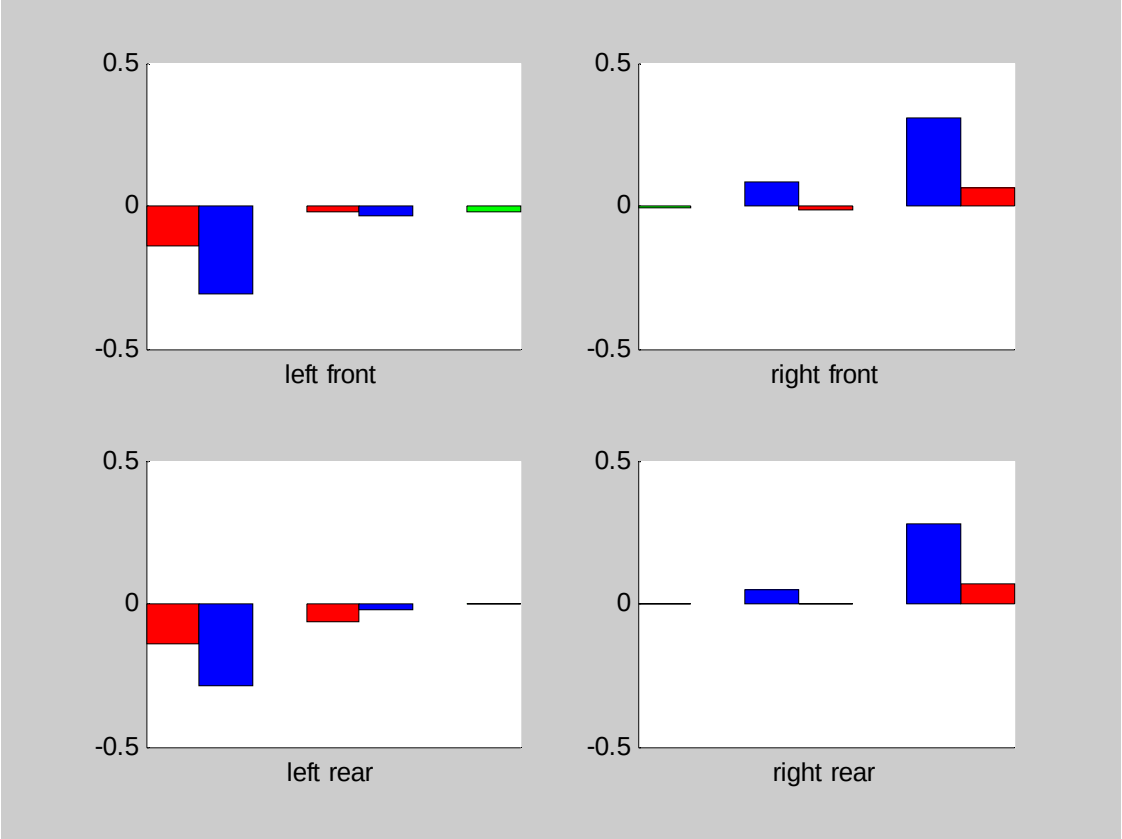

Figure 5.8. Effect of Rumble-strip Location on Measured Response for Rolled-in Case (mean RMS differences, right minus left)

Because of the simplicity and clarity on this conclusion, the investigation deviated from the initial plan, to focus more on validating the properties of these four sensors (outboard a_x), and also to decide whether wheel-speeds (available on the vehicle without additional sensing) could be used to provide an equivalent signal.. These issues are taken up in the following sections. For completeness additional factor effects are considered here via Figures 5.9 – 5.12.

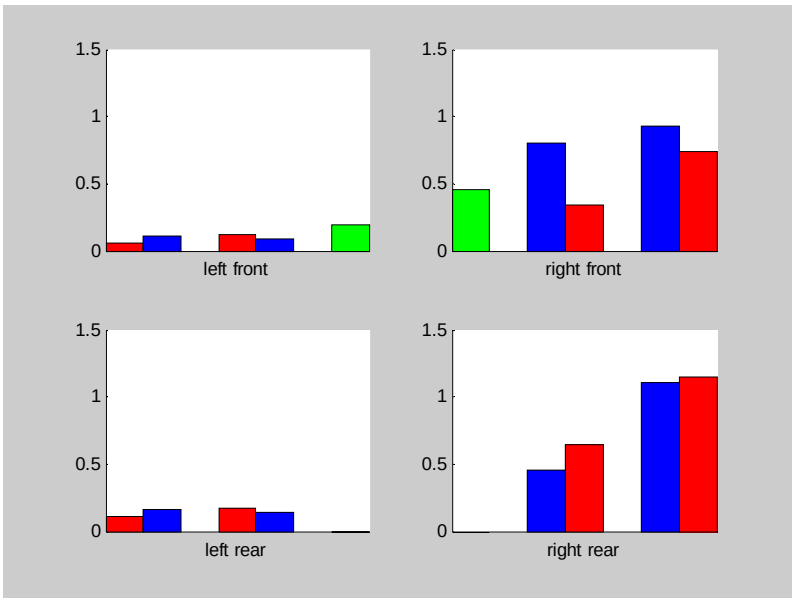

Figure 5.9. Effect of Rumble Strip Type (Milled – Rolled at 55mph)

Figure 5.9 considers the effect of rumble strip type – mean RMS responses for milled relative to mean RMS responses for rolled-in type. Note that all effects are positive – the milled rumble strip provides a significantly stronger signal, even on the non-excited side, and on the excited side the difference are very large, an observation that was also clear from Figures 5.6 and 5.7.

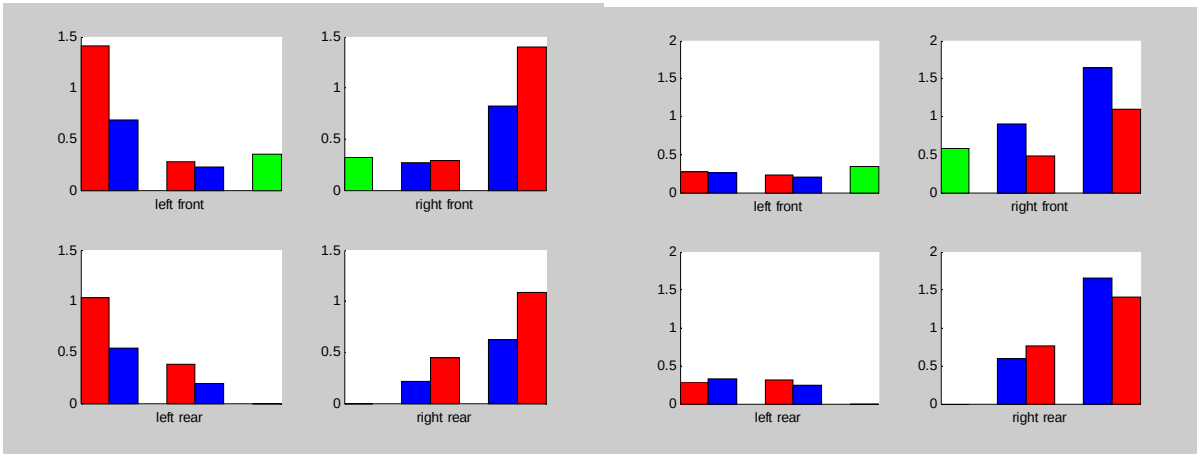

(a) (b)

Figure 5.10. Response on (a) Dirt Roads at 55mph compared with (b) Right Side Milled Shoulder Rumble-strips.

In Figure 10 the response amplitudes are in a similar range, the *pattern* of relative amplitudes is quite different between these cases, the dirt road providing a relatively large excitation in the a_z direction compared to a_x. Again, this provides further support for the idea that outboard a_x is the preferred single sensor measurement among those tested.

Figure 5.11 shows that selection of 4WD tends to reduce the response amplitude. The most obvious reason for this is the increase in effective inertia in the rotating wheel masses. This is interesting, because the vertical and longitudinal accelerations are similarly affected, while it might be presumed that the vertical accelerations would be influenced more directly by vertical tire stiffness, and would be relatively unaffected. This contradiction seems to imply that the rotational dynamics of the wheel are crucial to the response characteristics – for example a point follower tire model with bridging filter and vertical suspension dynamics would have difficulty predicting the vertical acceleration responses.

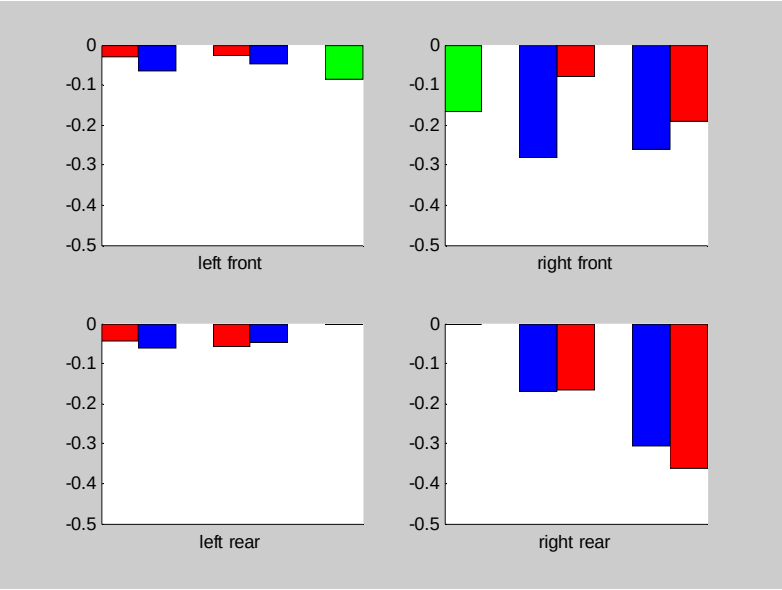

Figure 5.11. Effect of Transmission Selection on Response Amplitude (right side rumble strips, 4WD-2WD, 55mph only)

Given the effect of transmission selection on response, and the importance of rotational dynamics, the use of brakes would be expected to influence the responses. As shown in Figure 5.12, the effect of braking is actually small, except on the longitudinal acceleration on the side with the rumble-strip, and here it tends to amplify the response. Thus, for detection, the action of the brakes is not likely to inhibit the measured response, and in fact will tend to increase the amplitude of the outboard a_x signal.

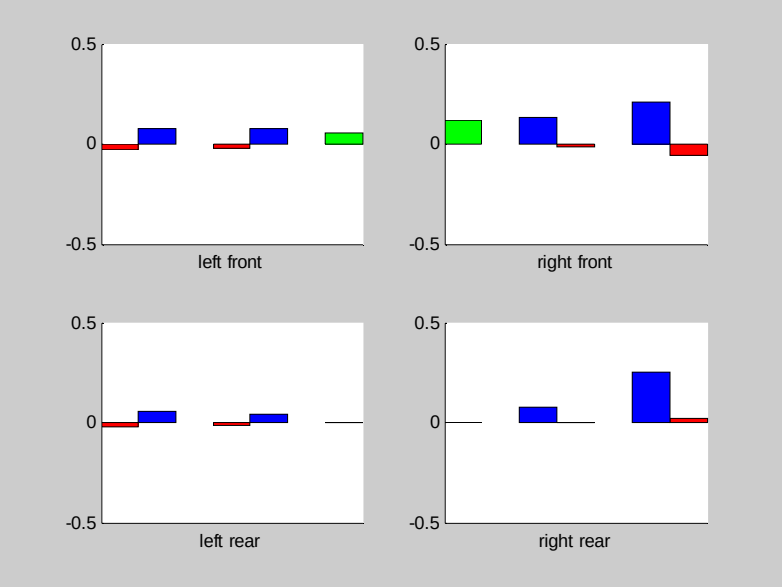

Figure 5.12. Effect of Braking on Response Amplitudes (right-side rumble strips, braking – coasting, 55 mph only)

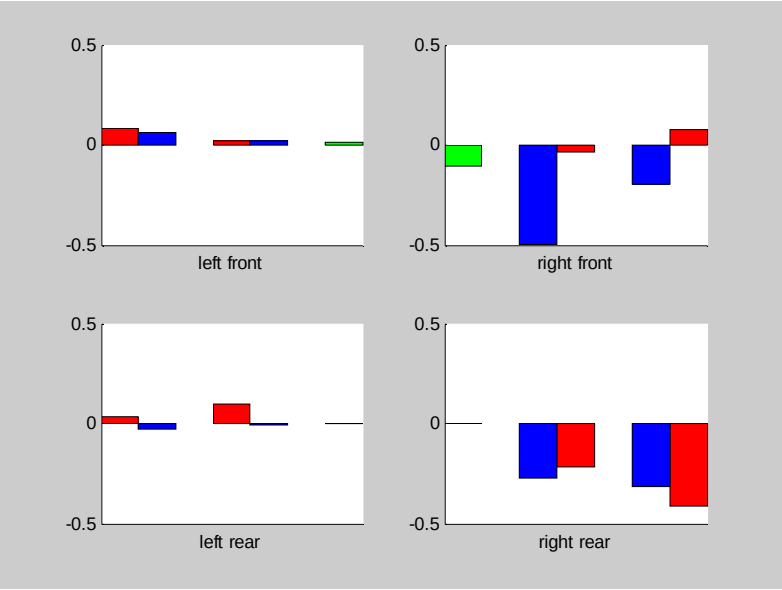

Figure 5.13. Effect of Speed (right sided rumble strips, cruising only, 70 mph -55 mph)

The comparison for speed in Figure 5.13 may seem counter-intuitive - amplitudes are smaller at higher speeds. However the detailed effects can be different, depending on the wavelength of the rumble strip (for runs with id 165 and 166 for example, the chassis-side a_x signal is actually higher for the 70 mph case). But the general trend is clear that the response amplitude are speed dependent, vary with the details of the excitation (as would be expected in a system which has resonant behavior), but at high speeds the response on the outboard a_x signal is slightly reduced.

5.3 Frequency Analysis of Outboard Longitudinal Accelerations

Based on the factor analysis, it now seems most reasonable to focus attention on the best detector we have – the outboard longitudinal accelerometer. We focus now on the frequency domain measures of this signal. Figure 5.14 shows the time history for outboard a_x signals on a right-side milled rumble strip, which quite clearly shows the relative amplitude. The corresponding power spectral density (PSD) is shown in Figure 5.15. Here the succession of peaks corresponds to harmonics of the fundamental frequency $\{f_0, 2f_0, 3f_0, ...\}$ mentioned in Section 4.1. The amplitudes may be less clear at first sight due to the logarithmic scales, but the peaks for the right side of the vehicle are at more than an order magnitude higher than on the left, and approximately two orders of magnitude higher than the background spectrum, which represents the resonance and filtering effects of the suspension on the broad-band road roughness characteristics. Note that some smaller harmonic peaks are visible on the left side, due to transmission through the chassis structure. The background roughness response is of similar amplitude on both sides, and from these two figures it seems clear that the sensors contain sufficient information to decide on the presence and lateral location of a rumble strip.

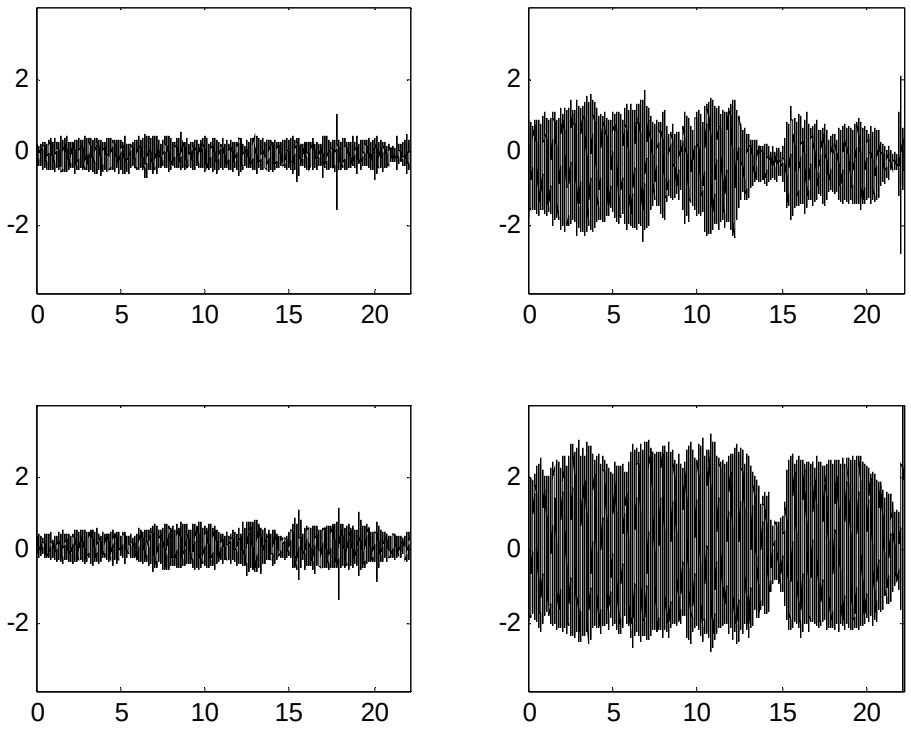

Figure 5.14. Time histories from Run 96 – right sided milled rumble strip

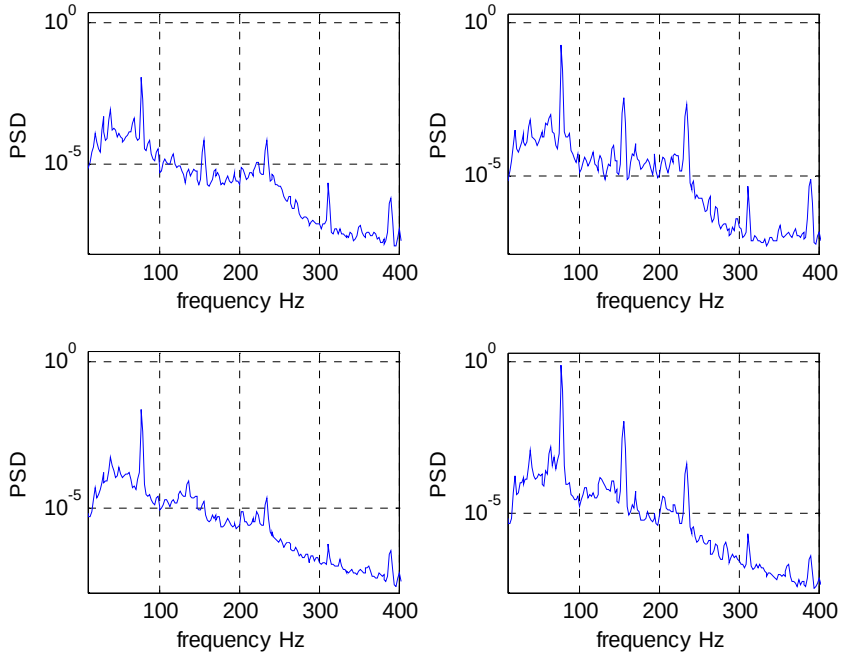

Figure 5.15. Frequency analysis (PSD) for Run 96. (milled, right side, semi-logarithmic plot)

Figure 5.16 shows very similar results for a rolled-in rumble strip, where again the presence of harmonic peaks, and their predominance on the right side of the vehicle, would be sufficient to trigger a decision that a rumble strip is present on the right side.

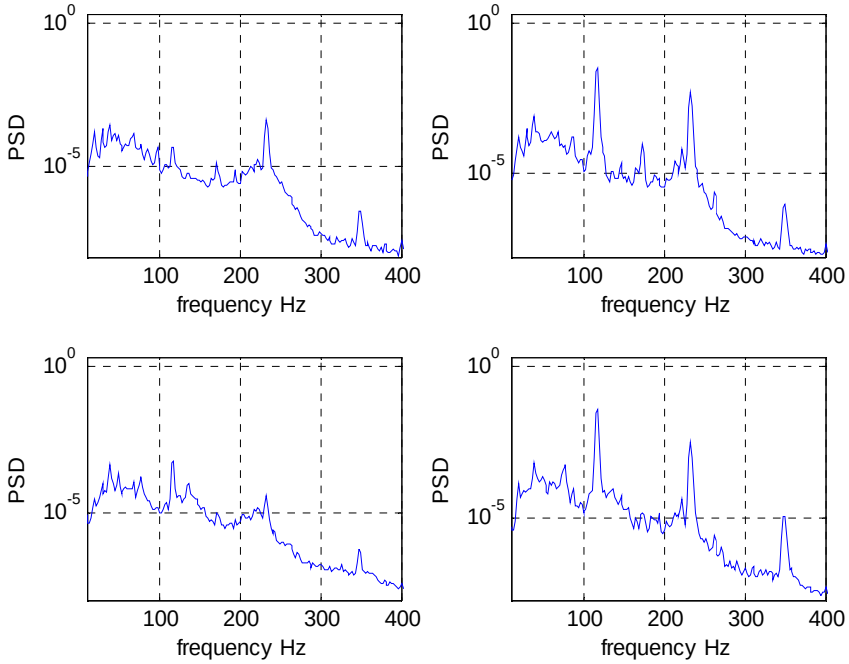

Figure 5.16. Frequency analysis (PSD) for Run 48. (rolled, right side, semi-logarithmic plot)

The following two plots (Figures 5.17 and 5.18) are on roads with no rumble strip contact, the first on a relatively smooth concrete road, the second on a relatively rough dirt road. Both show the same type of broad-band spectrum as was seen as background in the above plots, but neither shows a laterally biased pattern of harmonic peaks, or even any pattern of harmonic peaks at all. Thus is appears reasonable to hypothesize that a detection system could be based on (signal processing that extracts features equivalent to) this pattern of harmonic peaks, and it would not be triggered under normal driving conditions. Simply put, this type of vibration sensing, based on frequency, amplitude and lateral bias characteristics, seems to be able to extract the 'signature' of a rumble strip from the background disturbances from road roughness and indeed powertrain vibration.

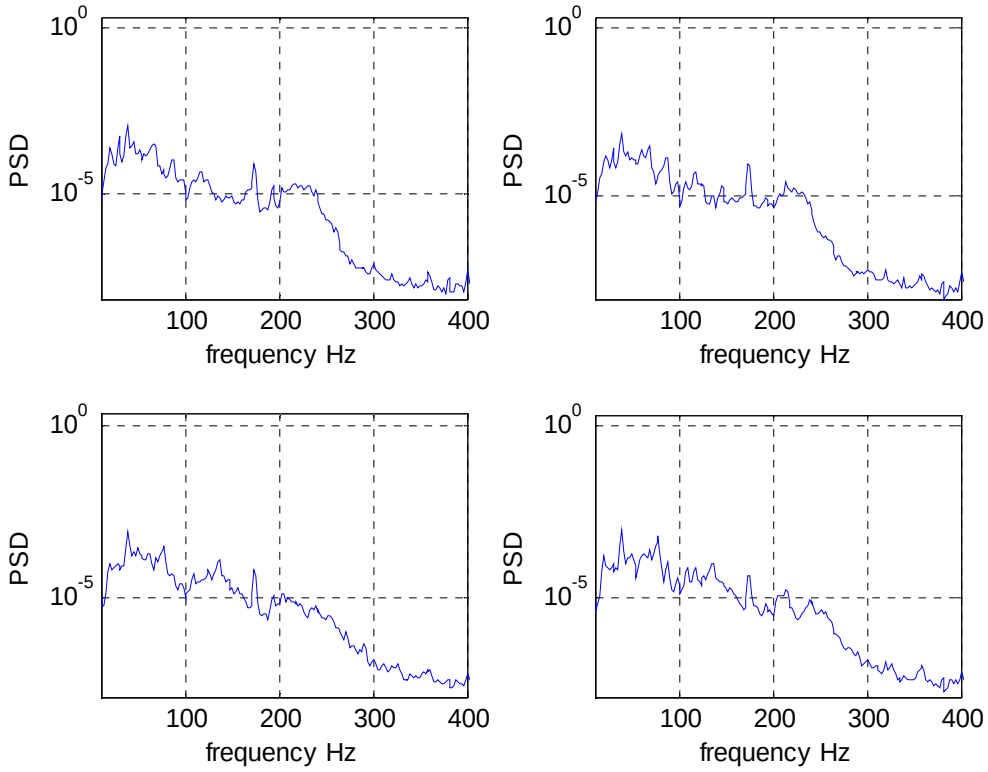

Figure 5.17 Frequency analysis (PSD) for Run 161 (smooth concrete road)

.

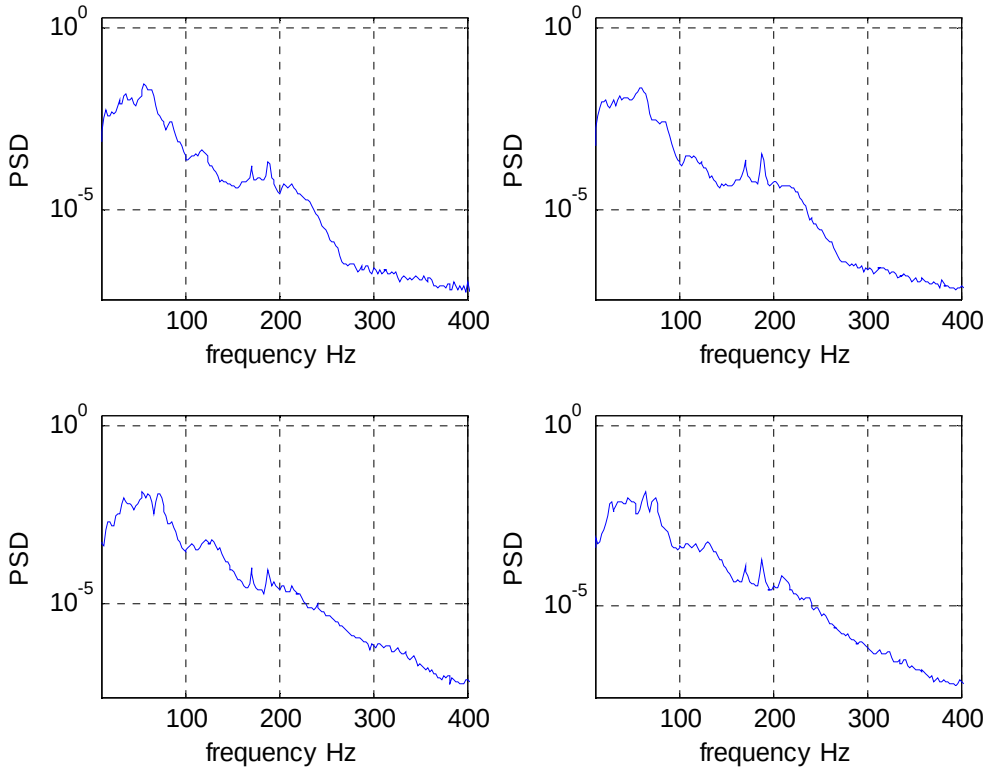

Figure 5.18. Frequency analysis (PSD) for Run 40 (dirt road, semi-logarithmic plot)

The above type of frequency plotting can be extended in the case of a coast-down test, where the speed dependence of the frequency plot can be seen. Figure 5.19 is an example of such a plot, where the vehicle coasts down on a concrete road, with no rumble strip contact. The basic shape of the PSD stays constant over time, as the speed decreases, and hence there is no evidence in road surface periodicity, as would be expected from a rumble strip. Figure 5.20 is the corresponding result from a rumble strip. The difference is very clear – there is now a pattern of harmonic peaks that decrease in frequency as the vehicle slows. These harmonics are evident in figure 5.21 (which is figure 5.20 viewed from "the top") where they are seen as straight lines that converge to [0,0]. This again gives a clear indication that the signal contains detailed information about the rumble strip that is causing a larger proportion of the vibration energy in the wheel hub vibration. Of course this is not surprising in any way, but the important conclusion is that any sensor that provides an equivalent signal to the longitudinal outboard accelerometer should be capable of reliably detecting a rumble strip.

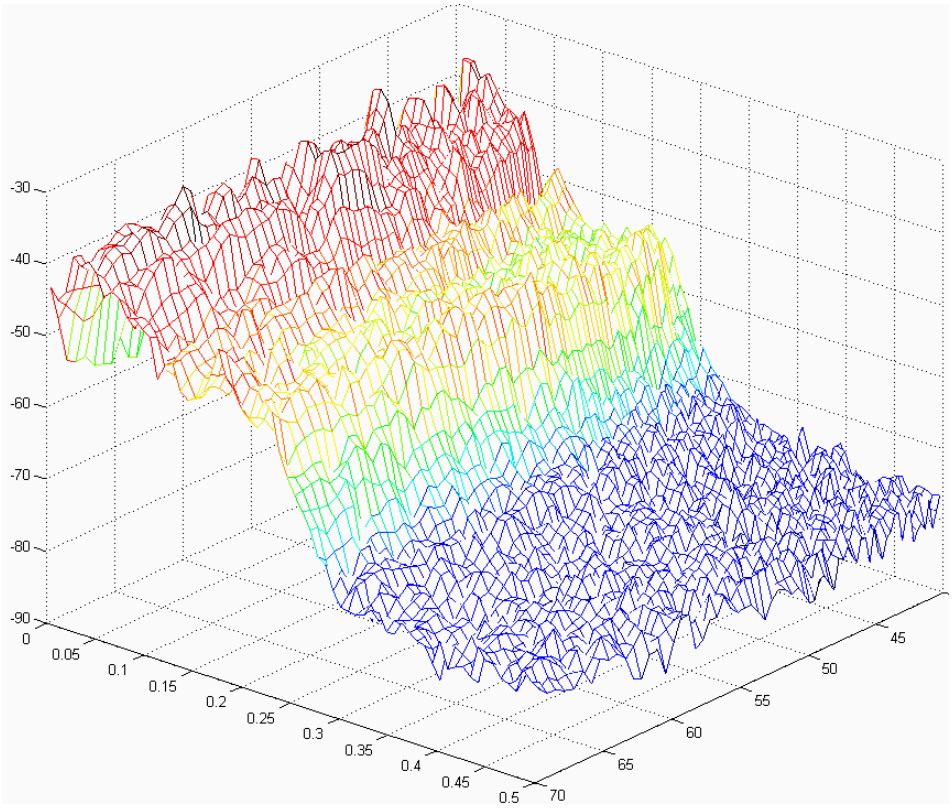

Figure 5.19. Waterfall plot of $a_{x\,wheel}(t)$ for the right front wheel on a concrete road (no rumble strip)

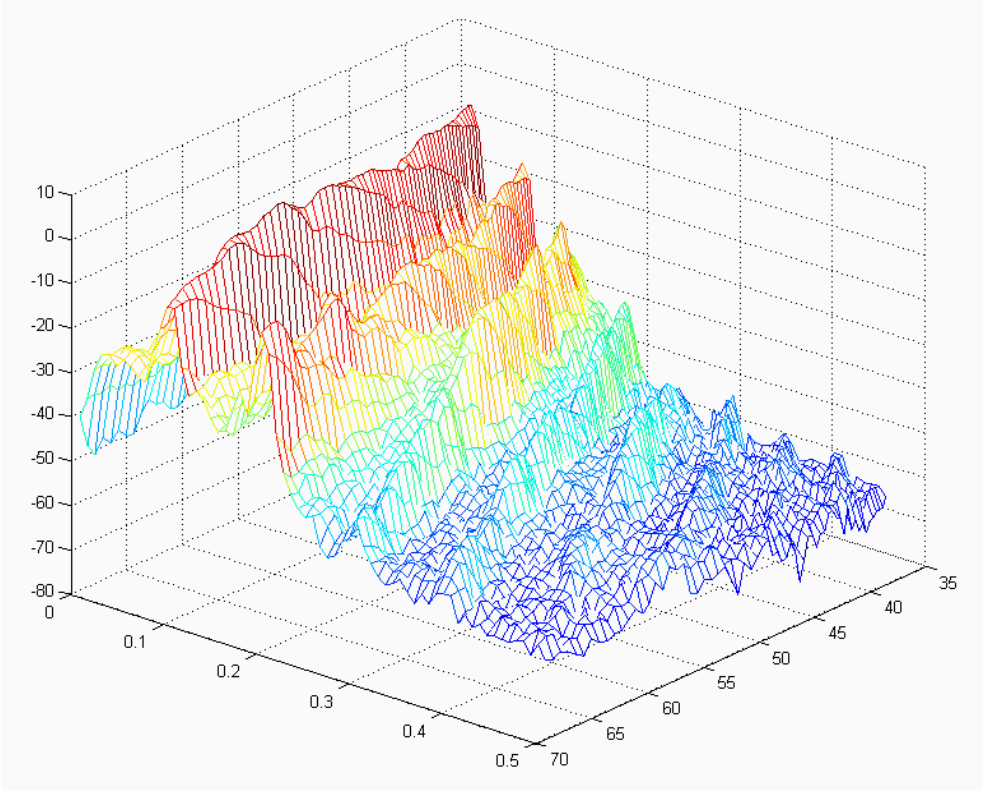

Figure 5.20. Waterfall plot of $a_{x\,wheel}(t)$ for the right front wheel in contact with a milled rumble strip

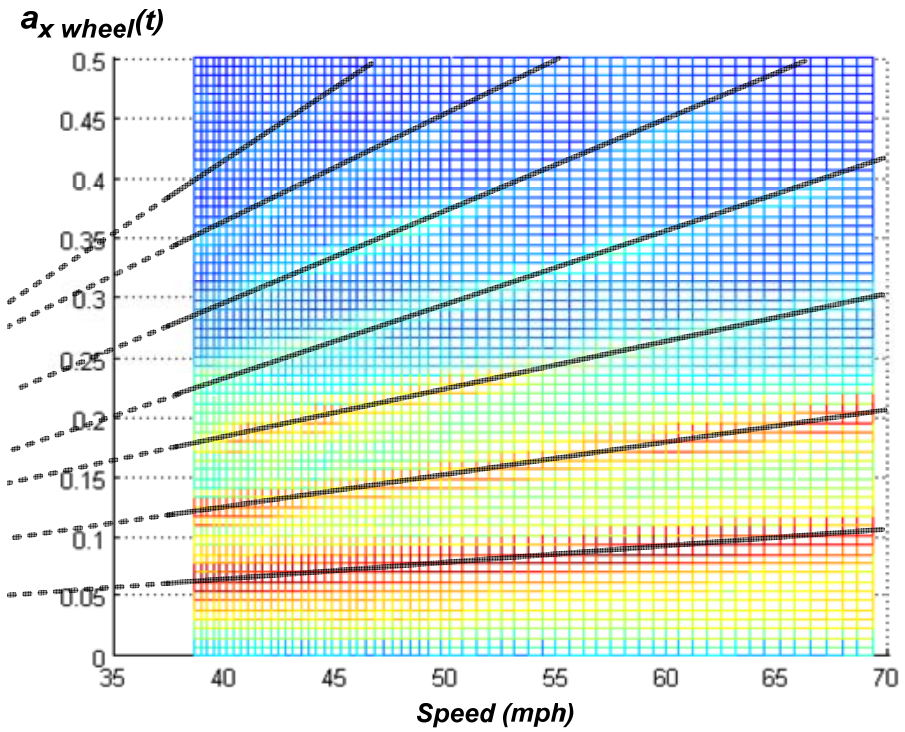

Figure 5.21. Harmonics in waterfall plot (of figure 5.20)

One further technique was employed to test the relationship between different sensors, namely the combination of coherency function and transfer function (frequency response) estimator. A typical coherency function is shown in Figure 5.22. A high degree of coherency should approach unity in the frequency range of interest, and generally this is not the case. In this plot, we see that the steering arm acceleration is not a good replacement (is not coherent with) the wheel mounted accelerometer. On a general rough road like this, the excitation is broad band, excites many of the vehicle and suspension resonances, and almost all sensors are poorly coherent, except possibly in a small frequency range – for example around 60Hz in Figure 5.22. In general we can conclude (from many figures similar to Figure 5.22) that no other sensor used in the study can be used as a direct substitute for the preferred $a_{x\,wheel}(t)$.

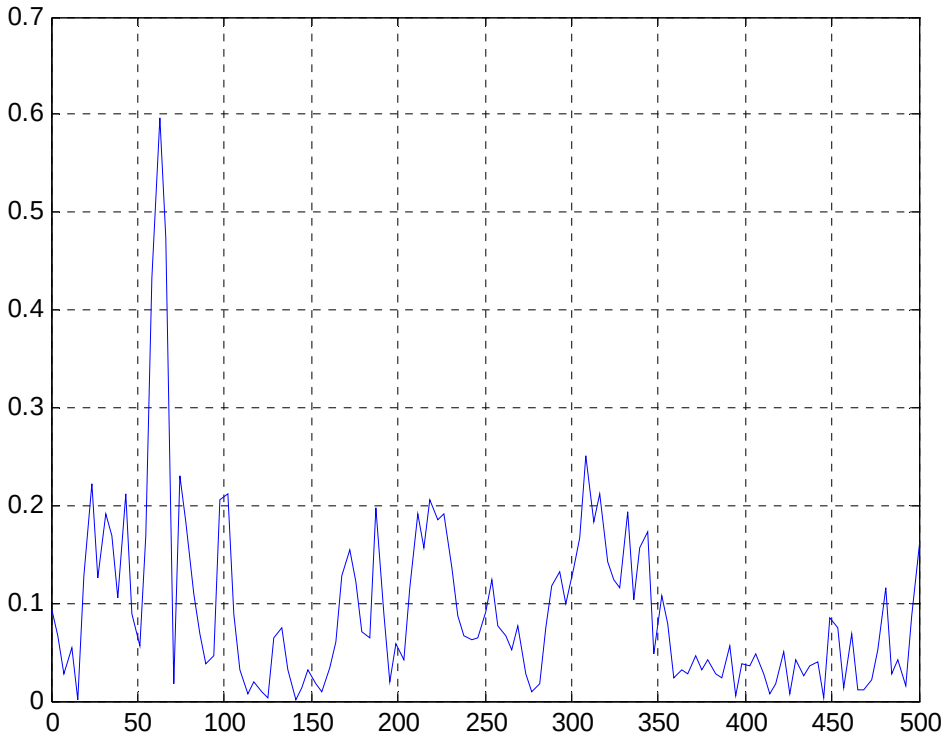

Figure 5.22. Coherency function between wheel (a_x) and steering sensor (a_y) mounted at the same wheel (front right wheel, excitation from dirt road - Run 40)

On the other hand, general coherency is not especially required. It is clearly more relevant to find signals that are coherent with $a_{x\,wheel}(t)$ *at the harmonic frequencies of interest under rumble-strip excitation*, provided that background effects are not in some way amplified. If so this would provide the basis of an alternative rumble strip sensing system. (Note: it is implicit here that other sensors may be easier, cheaper or more practical to install on a production vehicle; at this point no conclusion is made on whether $a_{x\,wheel}(t)$ could in reality be available, simply that if the same information could be found from alternative sources – especially those already available, such as wheel speed – then extra freedom exists in the design of a rumble strip detection system.

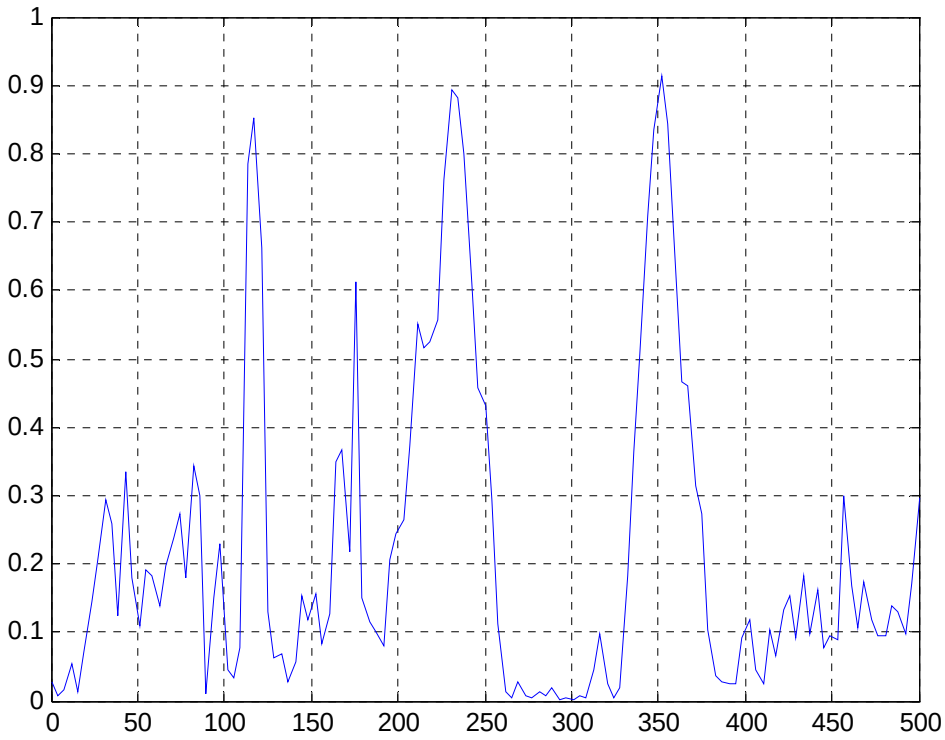

Figure 5.22. Coherency function between wheel (a_x) and steering sensor (a_y) mounted at the same wheel (front right wheel, excitation from rolled-in rumble strip - Run 90)

Figure 5.22 is an excellent example of how a separate sensor (lateral acceleration on the steering arm) can provide a potential substitute for the preferred sensor; the coherency is high around the harmonic peaks, and therefore the signal is directly related to the preferred $a_{x\,wheel}(t)$ measurement. However, we have already seen that directionality of response is relatively poor for the steering arm – which is hardly surprising given the very direct transmission path along the steering arm and steering rack – and indeed the left mounted accelerometer shows a very similar coherency in the above dataset.

Another sensor that may provide a more directionally sensitive replacement for $a_{x\,wheel}(t)$ is the wheel speed sensor, and this is considered in more detail in Section 6.

6. Wheel Speed Sensor Analysis

The wheel speed is measured by a series of voltage pulses, picked up by the 54 teeth mounted on each wheel. This pulse train provides timing triggers to the ABS system, which then computes a wheel-speed estimate for every control cycle – see Figure 6.1. To evaluate the likely validity of the wheel speed sensor for rumble strip detection we may look at time histories and amplitudes, but based on the analysis above it seems at least as appropriate to test whether the wheel speed is coherent with the reference signal $a_{x\,wheel}(t)$.

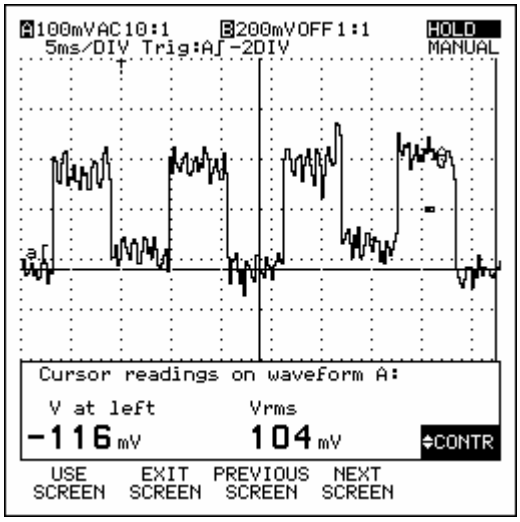

Figure 6.1. Direct analogue output measured on an oscilloscope from the existing wheel speed sensor.

Figure 6.2 shows a small section of the time history for a rolled-in rumble strip being detected by $a_{x\,wheel}(t)$. Figure 6.3 is the corresponding wheel speed estimate obtained from the CAN bus. There are two clear problems with the signal we see. First quantization error is large – the signal resolution appears to determined by the digital bit resolution of the underlying signal (wheel speed is shown in RPM units), so that variations due to wheel oscillation are not much larger than the quantization error itself. The second factor is that the signal is only updated every 15ms, independent of the speed of the vehicle, and thus there seems to be a severe loss of frequency bandwidth. In the example shown it is clear that the 15ms hold period is greater than cycle period, which is only 8ms.

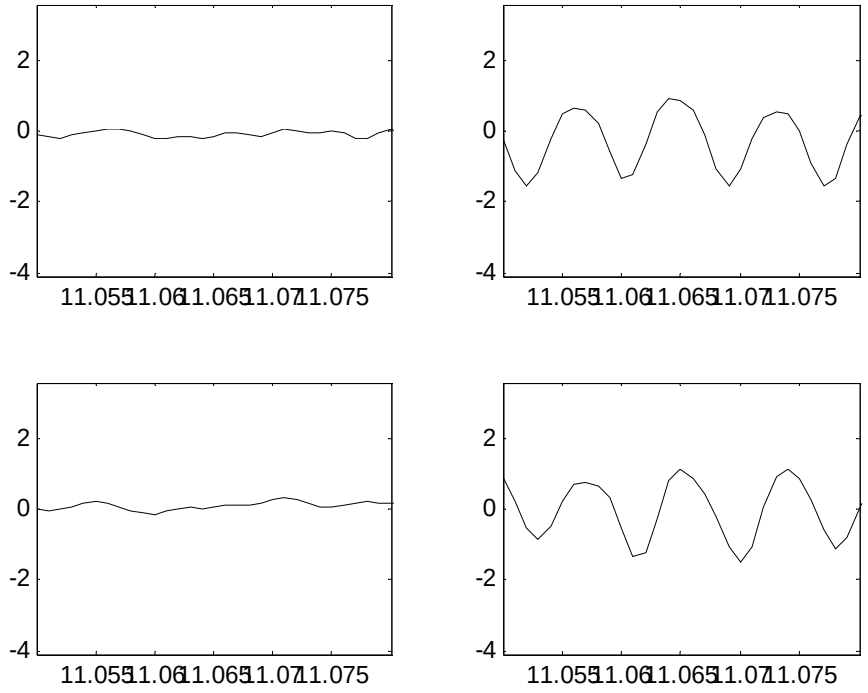

Figure 6.2. Reference accelerations ($a_{x\,wheel}(t)$) for Run 90 (rolled-in rumble strip response)

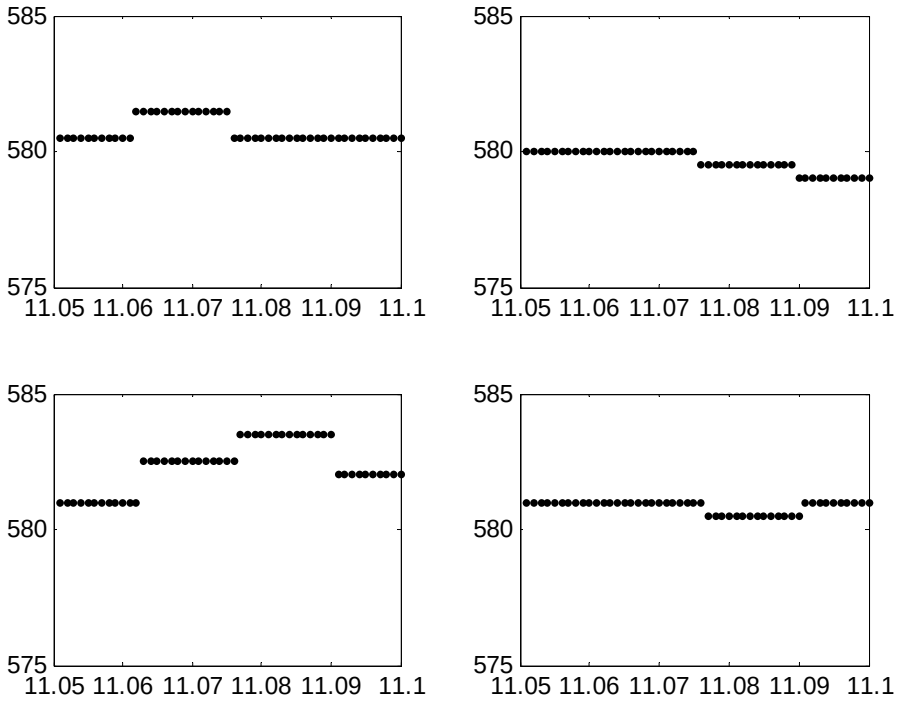

Figure 6.3. Wheel speed estimates from CAN data equivalent to Figure 6.2

We might conclude that the wheel speed sensor is not suitable, but two small pieces of analysis appear to indicate otherwise. Firstly, the loss of high frequency information is not fundamental, and is simply a feature of current signal processing for the ABS system. A simple analysis of the current example shows that the spatial period of the rumble strip is approximately 0.2m. The rolling radius of the tires on the test vehicle (larger than most!) is approximately 2.5m. There are 54 teeth on the wheel speed sensor and so counting positive and negative slope triggers there are $(0.2 \div 2.5) \times 2 \times 54 = 8.64$ measurement indicating wheel speed per rumble-strip cycle period, and this is independent of speed. Using the signal available from the CAN bus there are only 0.5 measurements per rumble-strip period.

The second indicator is that *in spite of the limitations of the available wheel speed sensor* it shows some degree of coherency with the reference signal. Figure 6.4 is the coherency plot that corresponds to Figure 5.22 above. In spite of the limitations of the signal as it currently exists, a coherent peak is clearly visible at around 120 Hz, as well as at lower frequencies.

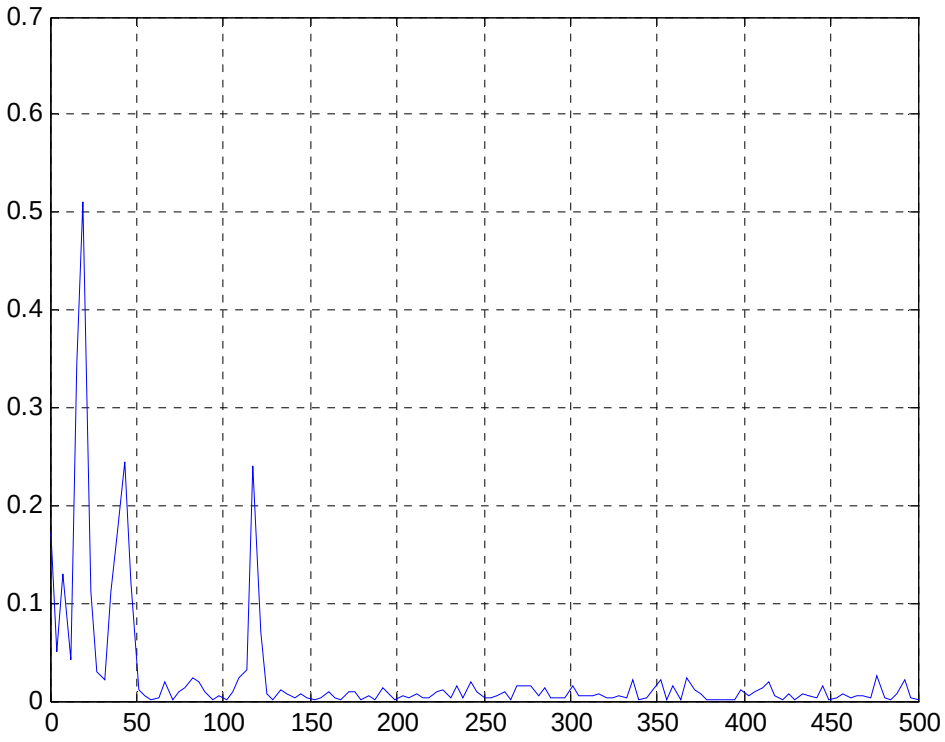

Figure 6.4. Coherency function between wheel (a_x) and available wheel-speed sensor (front right wheel, excitation from rolled-in rumble strip - Run 90)

Figure 6.5 shows another example based now on a milled rumble strip – this was selected to provide a stronger signal, perhaps overcoming some of the quantization problems noted above. It was also a lower speed case, driven at 40mph rather than the "standard" 55mph of run90 in the above figures. In this case the coherency approaches it maximum value of 1 near the excitation fundamental frequency, which is at about 60Hz in this case (the rumble strip has a longer wavelength than above, and the vehicle speed is of course reduced). Note also that the localization problem seen with the steering mounted accelerometer is not an issue here. For the same case (Run 168) as Figure 6.5, the other wheel speed shows no significant coherency at all, which is completely in contrast to the steering acceleration.

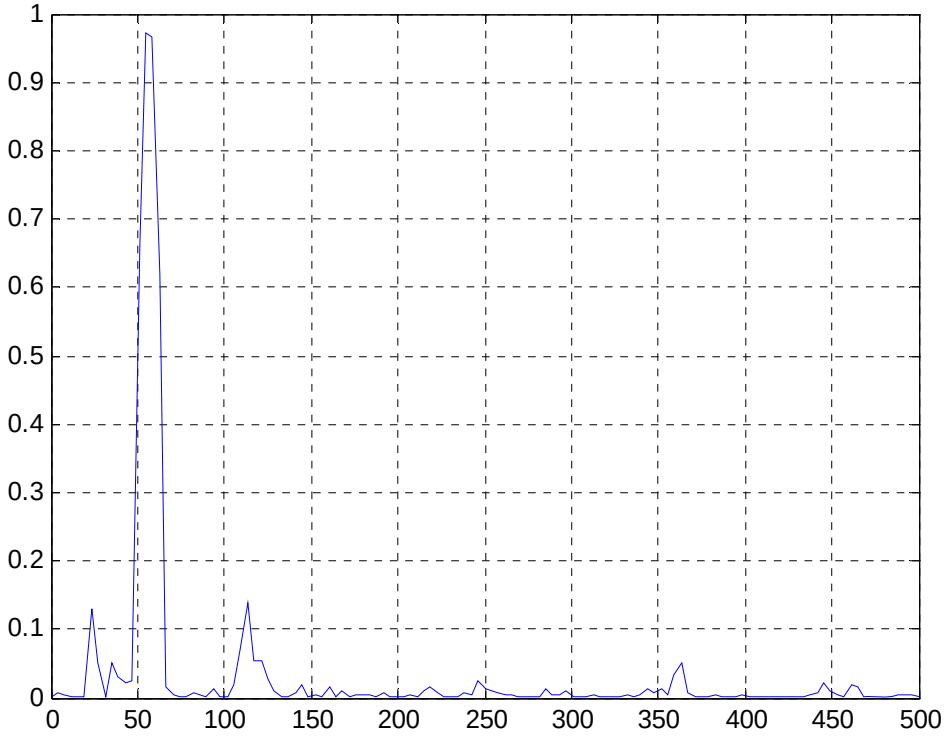

Figure 6.5. Coherency function between wheel (a_x) and available wheel-speed sensor (rear right wheel, excitation from milled rumble strip, 40mph, Run 168)

Thus in spite of the very limited quality of the available wheel speed sensor output, sample and held for 15 ms and quantized to very low resolution about the mean rotation speed, there is every indication that with alternative signal processing, the wheel speed oscillations could be used successfully as a sensor for rumble strip detection.

7. Conclusions

This report has considered the experimental analysis of vehicle vibration response from road surface features, in particular rumble strips. A sophisticated sensor and data acquisition system was fitted to a Nissan *Infiniti Q56* Sports Utility Vehicle, supported by simultaneous video and CAN data. Analysis of time histories, factor effects, power spectra and vibration transmission characteristics has led to the following conclusions:

- Both wheel (unsprung mass) and body (sprung mass) mounted accelerometers can detect the onset of a rumble strip; however body-mounted accelerometers are not reliable in terms of unambiguously detecting left/right position of the rumble strip – this is due to vibration transmission through the body structure, that depends on the detailed profile of the rumble strip.
- Rumble strips generate a clear lateral acceleration signature on the steering linkage, though directionality is again ambiguous.
- Of those sensors considered, wheel-mounted longitudinal accelerometers provide the best detection source for rumble strips. As evidenced by waterfall plots, these measurements
    - faithfully track the input
    - provide clear left/right directionality
    - detect the onset and departure from the rumble strip
    - are satisfactory on both milled and rolled strips
    - discriminate clearly from responses on other surfaces
- Transmission mode (4WD or 2WD) has a small effect on detecting rumble strips – 4WD tends to reduce the amplitude of the vibration response, but this does not affect the overall detectability using the preferred accelerometers.
- Wheel speeds obtained from the ABS module are coherent with the preferred accelerometer signal, but are corrupted by quantization and sample and hold processing in the ABS controller.
- Unprocessed wheel speeds provide a potential replacement for the wheel-mounted accelerometers. Further analysis indicates that the existing wheel speed sensor, with suitable processing of the analogue output signal could provide the basis of a robust and reliable detection system.
- Further experimentation using the same data acquisition system should be sufficient to determine eventual product feasibility.

Appendix A. Test Inventory: Summary of Data Collected

Road Type	Drive	Mode	Speed	Contact mode	Count
Smooth road	2WD	Cruise	40	N/A	2
			55		3
			70		2
		Coast	70		3
Cross lane	**Several runs made, details to follow**				
Dirt road	2WD	Cruise	55	N/A	1
		Coast	55		1
	4WD	Cruise	55		1
		Coast	55		1
Milled-in (3 sites)	2WD	Cruise	40	Full	4
			55		9
			55	Progressive	3
			70	Full	5
		Brake	55		2
		Coast	40		1
			55		6
			55	Progressive	4
			70	Full	4
		Accel	55		2
	4WD	Cruise	55		3
			55	Progressive	2
		Coast	55	Full	1
			55	Progressive	1
Rolled-in (2 sites)	2WD	Cruise	40	Full	4
			45		2
			50		1
			55		4
			55	Progressive	2
			60	Full	1
			65		1
			70		3
		Brake	55		2
		Coast	55		2
			55	Progressive	2
			70	Full	1
		Accel	55		3
	4WD	Cruise	40		2
			45		2
			55		3
			55	Progressive	3
			70	Full	5
		Coast	55		2
Intermitted	2WD	Cruise	40	Full	1
			55		2
			70		2
		Coast	40		1
			55		2
			70		2

Total: 116 runs

Appendix B. Data Catalog

Data catalog

RunId	Identified of rumble-strip data set
Time	Milliseconds into the run
AxLFChassis	Ax (m/sec^2) of left-front chassis accelerometer
AzLFChassis	Az (m/sec^2) of left-front chassis accelerometer
AxLFWheel	Ax (m/sec^2) of left-front wheel (suspension) accelerometer
AzLFWheel	Az (m/sec^2) of left-front wheel (suspension)accelerometer
AxRFChassis	Ax (m/sec^2) of right-front chassis accelerometer
AzRFChassis	Az (m/sec^2) of right-front chassis accelerometer
AxRFWheel	Ax (m/sec^2) of right-front wheel (suspension) accelerometer
AzRFWheel	Az (m/sec^2) of right-front wheel (suspension)accelerometer
AxLRChassis	Ax (m/sec^2) of left-rear chassis accelerometer
AzLRChassis	Az (m/sec^2) of left-rear chassis accelerometer
AxLRWheel	Ax (m/sec^2) of left-rear wheel (suspension) accelerometer
AzLRWheel	Az (m/sec^2) of left-rear wheel (suspension)accelerometer
AxRRChassis	Ax (m/sec^2) of right-rear chassis accelerometer
AzRRChassis	Az (m/sec^2) of right-rear chassis accelerometer
AxRRWheel	Ax (m/sec^2) of right-rear wheel (suspension) accelerometer
AzRRWheel	Az (m/sec^2) of right-rear wheel (suspension)accelerometer
AyLFSteer	Ay (m/sec^2) of left-side steering accelerometer
AyRFSteer	Ay (m/sec^2) of right-side steering accelerometer
Speed	mph
YawRate	Rad/sec
Ax	m/sec^s
Brake	0 or 1
Steer	degrees
SpeedLF	rpm or left-front wheel sensor
SpeedRF	rpm or right-front wheel sensor
SpeedLR	rpm or left-rear wheel sensor
SpeedRR	rpm or right-rear wheel sensor

Total size:

- Video: 1.09 GB, or about 6 MB per trip.
- Data: About 1 GB (950 MB).